Transmembrane Coordination of Preprotein Recognition and Motor Coupling by the Mitochondrial Presequence Receptor Tim50

Anne Caumont-Sarcos, Cyril Moulin, Lucyle Poinot, Bernard Guiard, Martin van Der Laan, Raffaele Ieva

Article

Cell Reports

Transmembrane Coordination of Preprotein Recognition and Motor Coupling by the Mitochondrial Presequence Receptor Tim50

Graphical Abstract

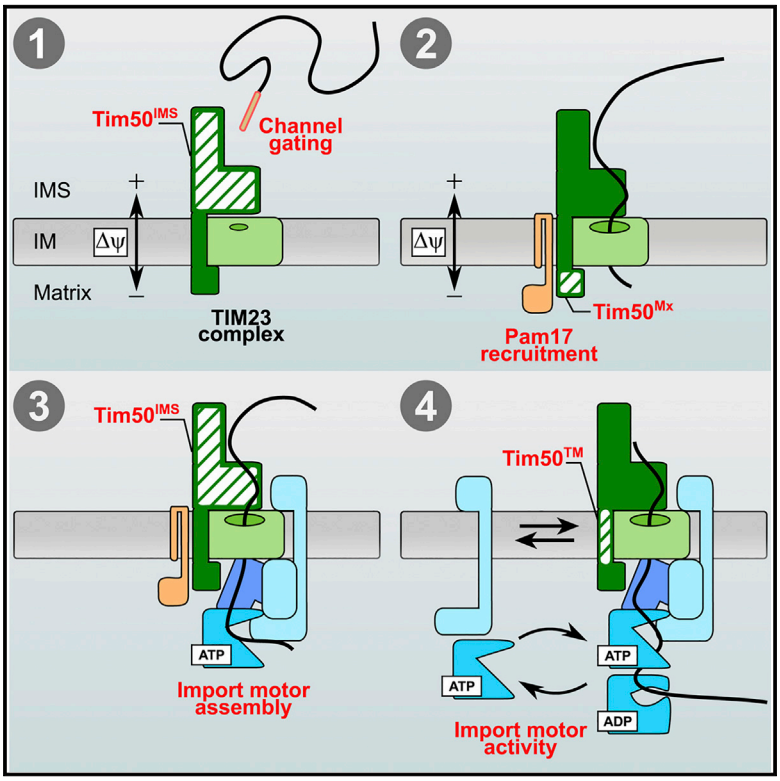

Highlights

- The receptor Tim50 couples preprotein recognition to import motor activation
- Tim50 matrix domain promotes recruitment of Pam17 to TIM23
- Tim50 intermembrane space domain licenses import motor assembly
- Tim50 transmembrane segment stimulates import motor activity

Authors

Anne Caumont-Sarcos, Cyril Moulin, Lucyle Poinot, Bernard Guiard, Martin van der Laan, Raffaele Ieva

Correspondence

martin.van-der-laan@uks.eu (M.v.d.L.), raffaele.ieva@ibcg.biotoul.fr (R.I.)

In Brief

Caumont-Sarcos et al. report a transmembrane coordination mechanism that promotes import of presequence-containing preproteins into mitochondria. The presequence translocase subunit Tim50 links the preprotein receptor function on the *cis* side of the mitochondrial inner membrane to functional activation of the import motor on the *trans* side.

Caumont-Sarcos et al., 2020, Cell Reports *30*, 3092–3104
March 3, 2020
https://doi.org/10.1016/j.celrep.2020.02.031

CellPress

OPEN ACCESS
CellPress

Cell Reports
Article

Transmembrane Coordination of Preprotein Recognition and Motor Coupling by the Mitochondrial Presequence Receptor Tim50

Anne Caumont-Sarcos,[1,5] Cyril Moulin,[1,5] Lucyle Poinot,[1] Bernard Guiard,[2] Martin van der Laan,[3,*] and Raffaele Ieva[1,4,6,*]
[1]Laboratoire de Microbiologie et Génétique Moléculaires, Centre de Biologie Intégrative (CBI), Université de Toulouse, CNRS, UPS, Toulouse 31062, France
[2]Centre de Génétique Moléculaire, CNRS, Gif-sur-Yvette 91190, France
[3]Medical Biochemistry & Molecular Biology, Center for Molecular Signaling, PZMS, Faculty of Medicine, Saarland University, Homburg 66421, Germany
[4]Institute of Biochemistry and Molecular Biology, ZBMZ, Faculty of Medicine, University of Freiburg, Freiburg 79104, Germany
[5]These authors contributed equally
[6]Lead Contact
*Correspondence: martin.van-der-laan@uks.eu (M.v.d.L.), raffaele.ieva@ibcg.biotoul.fr (R.I.)
https://doi.org/10.1016/j.celrep.2020.02.031

SUMMARY

Mitochondrial preproteins contain amino-terminal presequences directing them to the presequence translocase of the mitochondrial inner membrane (TIM23 complex). Depending on additional downstream import signals, TIM23 either inserts preproteins into the inner membrane or translocates them into the matrix. Matrix import requires the coupling of the presequence translocase-associated motor (PAM) to TIM23. The molecular mechanisms coordinating preprotein recognition by TIM23 in the intermembrane space (IMS) with PAM activation in the matrix are unknown. Here we show that subsequent to presequence recognition in the IMS, the Tim50 matrix domain facilitates the recruitment of the coupling factor Pam17. Next, the IMS domain of Tim50 promotes PAM recruitment to TIM23. Finally, the Tim50 transmembrane segment stimulates the matrix-directed import-driving force exerted by PAM. We propose that recognition of preprotein segments in the IMS and transfer of signal information across the inner membrane by Tim50 determine import motor activation.

INTRODUCTION

The majority of mitochondrial precursor proteins (preproteins) are imported into the organelle by means of amino (N)-terminal, positively charged α-helical signals called presequences (Vögtle et al., 2009). These signals target preproteins to the translocase of the outer mitochondrial membrane (TOM complex) and to the presequence translocase of the inner membrane (TIM23 complex) (Chacinska et al., 2009; Endo and Yamano, 2009; Mokranjac and Neupert, 2009; Marom et al., 2011; Schulz et al., 2015; Hansen and Herrmann, 2019; Pfanner et al., 2019). After transport by the TIM23 complex into the matrix, the preprotein N termini are proteolytically removed by the mitochondrial processing peptidase (MPP) (Teixeira and Glaser, 2013; Poveda-Huertes et al., 2017). Additional sorting signals that are carboxy (C)-terminal to the matrix-targeted presequence element determine the ultimate sub-mitochondrial localization of each preprotein. Whereas largely water-soluble preproteins are transported into the matrix, a substantial number of preproteins contain hydrophobic stop-transfer signals that are released into the lipid bilayer via an ill-defined lateral gate of the TIM23 complex (Dudek et al., 2013; Glick et al., 1992; Ieva et al., 2014; Mokranjac and Neupert, 2010; Moulin et al., 2019; Schendzielorz et al., 2018).

Three essential subunits constitute the central core of the presequence translocase. The multi-spanning membrane protein Tim23 forms a channel that is activated by the membrane potential ($\Delta\psi$) and gated by the presequence signal. Tim17 is homologous to Tim23 and regulates its channel activity (Dekker et al., 1997; Milisav et al., 2001; Truscott et al., 2001; Martinez-Caballero et al., 2007; Popov-Celeketić et al., 2008; Ramesh et al., 2016; Wrobel et al., 2016; Filipuzzi et al., 2017; Matta et al., 2017). The single-membrane span Tim50 subunit functions as a preprotein receptor and promotes $\Delta\psi$- and presequence-dependent gating of the polypeptide transport channel (Meinecke et al., 2006; Lytovchenko et al., 2013). The $\Delta\psi$ across the inner membrane suffices in driving both the electrophoretic transport of the positively charged residues of the presequence into the matrix (Martin et al., 1991; Turakhiya et al., 2016) and the lateral sorting of stop-transfer signals into the membrane (van der Laan et al., 2007). Translocation of mature polypeptide segments into the matrix requires both the $\Delta\psi$ and the presequence translocase-associated import motor (PAM) machinery (Mokranjac and Neupert, 2010; Dudek et al., 2013; Schulz et al., 2015; Demishtein-Zohary and Azem, 2017; Craig, 2018). The inward-directed driving force exerted by the PAM machinery is generated by matrix-localized mitochondrial Hsp70 (mtHsp70) that hydrolyzes adenosine triphosphate (ATP) to cyclically bind polypeptide segments as they emerge on the matrix exit side of the TIM23 protein translocating channel (Ungermann et al., 1994; Voos et al., 1996; Voisine et al., 1999; Liu et al., 2003; Schulz and Rehling, 2014). Positioning of mtHsp70 at the translocase

and its ATP hydrolysis cycles are tightly coordinated by several co-chaperones via multiple protein-protein interactions. The Tim44 subunit directly interacts with the matrix side of the Tim23-Tim17 core of the translocase, thus functioning as a platform for the assembly of mtHsp70 and its co-chaperones (Blom et al., 1993; Horst et al., 1993; Schneider et al., 1994; Liu et al., 2003; Hutu et al., 2008; Ting et al., 2014, 2017; Banerjee et al., 2015). The matrix-localized J-domain of the Pam18 co-chaperone together with the J-like protein Pam16 regulates the ATPase activity of mtHsp70 (D'Silva et al., 2003, 2005; Mokranjac et al., 2003b; Truscott et al., 2003; Frazier et al., 2004; Kozany et al., 2004). The initial step of PAM recruitment to import sites is facilitated by the transient association of the regulatory component Pam17 to the TIM23 complex (van der Laan et al., 2005; Hutu et al., 2008; Popov-Celeketić et al., 2008; Schiller, 2009; Lytovchenko et al., 2013). It remains unclear how the assembly of import motor subunits and the cyclic activity of the PAM machinery are adapted to the polypeptide segments that transit through the TIM23 complex, thus ensuring that only matrix-targeted segments are "pulled" into the matrix.

Although the receptor, channel, and motor modules of the TIM23/PAM machinery have been characterized to some extent, we know very little about the signal-driven coordination of their activities and thus the regulation of preprotein import. The intermembrane space (IMS) domain of Tim50 ($Tim50^{IMS}$) is sufficient for presequence recognition (Meinecke et al., 2006; Mokranjac et al., 2009). A C-terminal presequence binding domain (PBD) was mapped between residues 395 and 476 in $Tim50^{IMS}$ (Schulz et al., 2011; Rahman et al., 2014). In addition, the core domain of $Tim50^{IMS}$ (residues 164–361) contains a putative peptide binding groove in close proximity to the channel-forming subunit Tim23 (Qian et al., 2011; Rahman et al., 2014). By acting as a preprotein receptor, the Tim50 IMS domain plays an early role in import. Sites of interaction between the Tim50 IMS domain and the Tim23 subunit promote the handover of preproteins from TOM to TIM23 and influence the subsequent steps of the import reaction (Geissler et al., 2002; Yamamoto et al., 2002; Chacinska et al., 2003; Mokranjac et al., 2003a; Tamura et al., 2009; Shiota et al., 2011; Waegemann et al., 2015). Thus, presequence recognition and transfer to TIM23 represent critical steps for the onset of both the inner membrane sorting and the PAM-dependent matrix-targeting pathways. Oddly enough, however, partial depletion of Tim50 most predominantly impairs import of preproteins targeted to the matrix (Geissler et al., 2002; Yamamoto et al., 2002; Mokranjac et al., 2003a; Tamura et al., 2009). Whereas this apparent conundrum remains unresolved, it was recently shown that Tim50 promotes the recruitment of Pam17 to the TIM23 complex, identifying an important link between Tim50 and matrix translocation (Schendzielorz et al., 2017). Notably, this study uncovered an additional function of Pam17 in promoting the $\Delta\psi$-dependent import of mature polypeptide segments, which occurs after $\Delta\psi$-dependent matrix translocation of the presequence signal (Schendzielorz et al., 2017).

In contrast to the extensively characterized Tim50 IMS domain, the functions of the Tim50 N-terminal moiety, composed of the water-soluble matrix domain ($Tim50^{Mx}$) and the transmembrane segment ($Tim50^{TM}$), are unknown. In this study, we reveal an unexpected role of the N-terminal portion of Tim50 in promoting cell viability under growth conditions that require particularly high mitochondrial activity. We show that $Tim50^{Mx}$ and $Tim50^{TM}$ function in coordination with $Tim50^{IMS}$ and that all three Tim50 domains fulfill specific regulatory roles during matrix translocation of preproteins segments. Upon presequence recognition at the TIM23 complex, the $Tim50^{Mx}$ specifically promotes the recruitment of Pam17 to the translocase. Subsequently, $Tim50^{IMS}$ licenses docking of PAM components to the TIM23 complex. Finally, $Tim50^{TM}$ determines the import-driving activity of PAM. Taken together, our findings uncover Tim50 as a central coordinator that regulates the multi-step matrix import reaction by transducing distinct stimuli across the mitochondrial inner membrane to the PAM machinery.

RESULTS

The Matrix and Transmembrane Domains of Tim50 Promote Efficient Preprotein Import

Previous studies have suggested that Tim50, in addition to presequence recognition, may play a regulatory role at late steps of the import reaction (Tamura et al., 2009; Schendzielorz et al., 2017), but the molecular basis of this putative function is unknown. In a screen for Tim50 subdomains that may influence late preprotein import steps, we generated *Saccharomyces cerevisiae tim50* mutant alleles encoding two truncated forms of Tim50, both possessing the intact IMS PBD (Figure 1A). In one strain, termed *tim50*$^{TM/IMS}$, a large portion of $Tim50^{Mx}$ was deleted by fusing the presequence of Tim50 directly upstream of its transmembrane segment (Figure S1). In a second strain, termed *tim50*^{IMS}, only the IMS domain was expressed and targeted to mitochondria by fusion to the bipartite presequence of cytochrome b_2 (Cyb2; Figure S1). In the resulting fusion protein, the matrix-targeting Cyb2 presequence is cleaved off by MPP in the matrix. The following hydrophobic stop-transfer segment is laterally sorted into the inner membrane and subsequently removed by the inner membrane protease (IMP). Thus, the C-terminally fused water-soluble Tim50 domain is released into the IMS. On synthetic medium containing lactate as a predominant carbon source, a growth condition that requires a particularly high mitochondrial activity, the *tim50* mutant strains revealed a growth defect at 37°C, but not at lower temperatures (Figure 1B; Figures S2A and S2B). The conditional growth defect was most severe for the mutant strain lacking both the matrix domain and the transmembrane segment of Tim50. This result was surprising, because it has been previously reported that $Tim50^{IMS}$ is sufficient to promote presequence recognition and preprotein import by the TIM23 complex (Meinecke et al., 2006; Mokranjac et al., 2009; Schulz et al., 2011; Malhotra et al., 2017).

To investigate the effect of Tim50 truncations on the presequence import pathway, we isolated mitochondria from wild-type and mutant cells cultured at 24°C (Figure S2A). The steady-state levels of mitochondrial proteins were unaltered under these permissive conditions (Figure S2C). The import of radiolabeled ADP/ATP carrier protein (AAC), which is independent of the TIM23 complex (Kang et al., 2018), was similarly efficient in wild-type and mutant mitochondria (Figure S2D). In addition,

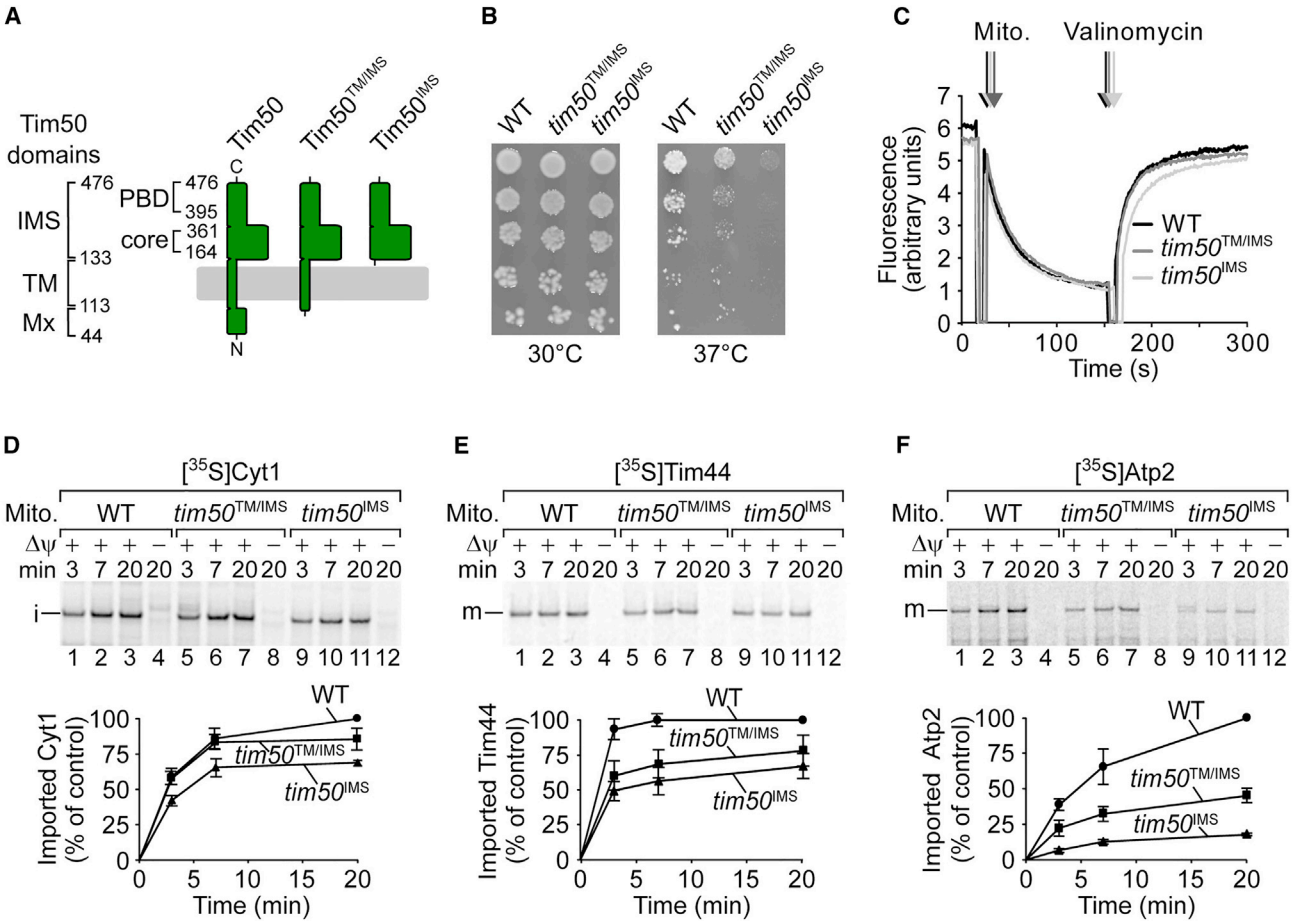

Figure 1. The N-Terminal Moiety of Tim50 Promotes Preprotein Import into the Matrix

(A) Schematic representation of Tim50 truncation protein variants. IMS, intermembrane space; TM, transmembrane segment; Mx, matrix; PBD, presequence binding domain. The amino acid positions delimiting the indicated protein domains are reported.

(B) Serial dilutions of strains expressing either wild-type or the indicated truncated forms of *TIM50* on synthetic defined medium containing lactate at 30°C or 37°C.

(C) Measurement of the membrane potential ($\Delta\psi$) of isolated mitochondria on the basis of quenching of the potential sensitive fluorescent dye 3,3′-dipropylthiadicarbocyanine iodide. The mitochondrial $\Delta\psi$ is proportional to the gain of fluorescence measured upon its uncoupling with valinomycin. Arrows indicate the addition of mitochondria (Mito.) and valinomycin.

(D–F) Radiolabeled Cyt1 (D), Tim44 (E), or Atp2 (F) were imported into wild-type or truncated *tim50* mitochondria. The amounts of MPP-processed and Proteinase K-resistant proteins were quantified for each time point and normalized to the corresponding protein amounts imported into wild-type mitochondria after the longest period of time. Data are plotted as mean ± SEM (n = 3). i, intermediate; m, mature.

See also Figures S1 and S2.

lack of the Tim50 matrix and TM domains did not cause dissipation of the mitochondrial $\Delta\psi$ across the inner mitochondrial membrane, as judged by the uptake of the $\Delta\psi$-sensitive dye 3,3′-dipropylthiadicarbocyanine iodide into mitochondria (Figure 1C). We conclude that the TIM23 channel-gating function of Tim50 is intact in these mutant strains, which is in agreement with the notion that the recombinant, purified Tim50^{IMS} domain is sufficient to induce gating transitions of a channel formed by the Tim23 protein (Meinecke et al., 2006). Thus the conditional growth defects of *tim50*$^{TM/IMS}$ and *tim50*^{IMS} strains point to a so far unexplored regulatory role of the Tim50 N-terminal moiety during preprotein import that is required for cell growth under stringent conditions. To further explore this scenario, *in vitro* synthesized and radiolabeled model preproteins were incubated with isolated mitochondria. Import of the inner membrane-sorted cytochrome c_1 (Cyt1) subunit of the cytochrome bc_1 complex occurred with wild-type-like efficiency in *tim50*$^{TM/IMS}$ and was moderately impaired in *tim50*^{IMS} mitochondria (Figure 1D). Import of matrix-targeted Tim44 was partially defective in the *tim50*-mutant mitochondria (Figure 1E). This defect was most obvious at early and intermediate time points of the import reaction, suggesting impaired kinetics of import. Notably, import of the matrix-localized subunit β of the F_1F_o ATP synthase complex, Atp2, was strongly inhibited at all time points assessed in both mutant mitochondria (Figure 1F). We conclude that the N-terminal domains of Tim50 support translocation of polypeptide

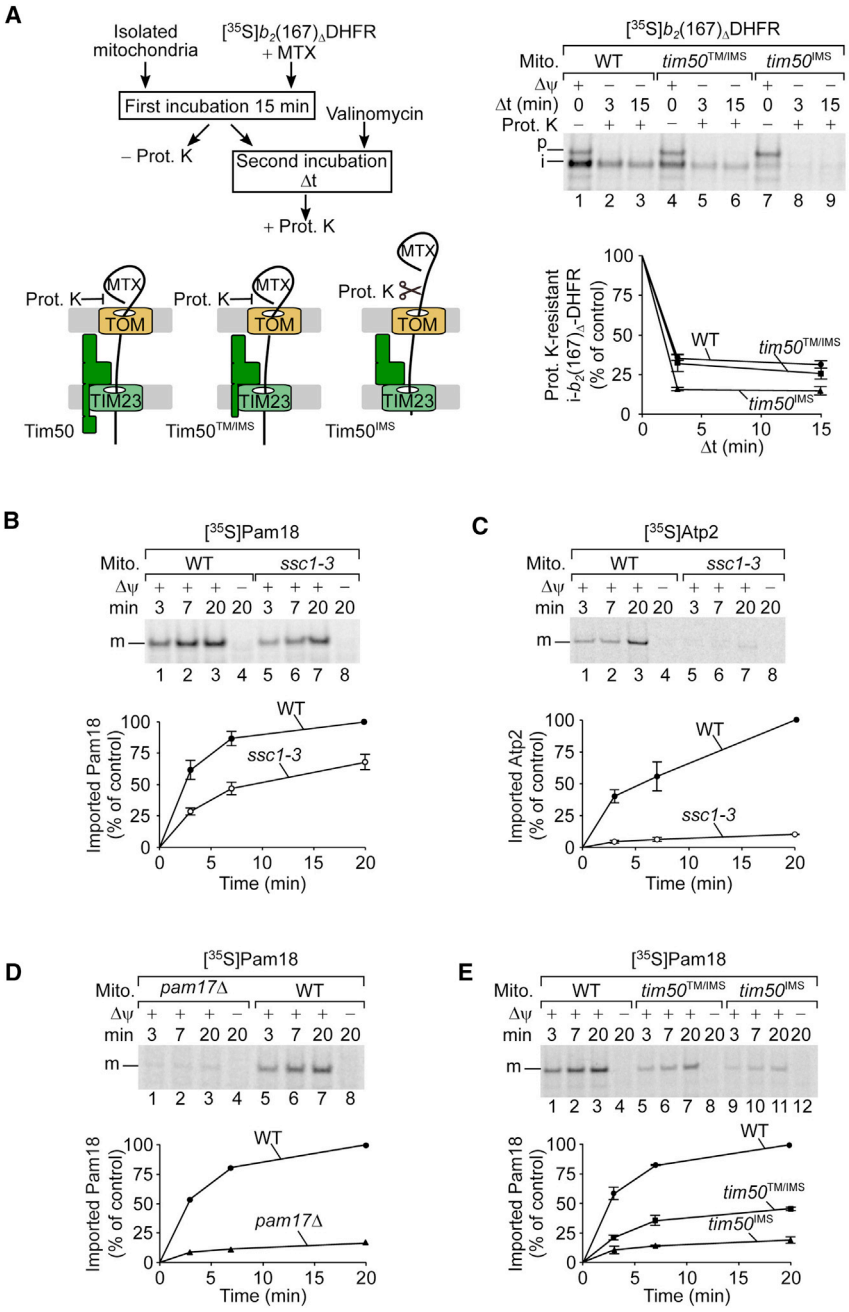

Figure 2. The N-Terminal Moiety of Tim50 Promotes Pam17- and Motor-Dependent Import

(A) The import-driving activity exerted by the PAM machinery was estimated for wild-type and the indicated mutant mitochondria. Radiolabeled $b_2(167)_\Delta$-DHFR was first accumulated at mitochondrial import sites for 15 min in the presence of methotrexate. After addition of valinomycin to uncouple the membrane potential, the radiolabeled protein was chased up to 15 additional minutes (Δt). The relative amount of MPP-processed intermediate protein i-$b_2(167)_\Delta$-DHFR, which is Proteinase K resistant, over the total amount of i-$b_2(167)_\Delta$-DHFR at the start of the chase phase was quantified. The amount of intermediate that formed after the pulse phase was set to 100%. Data are plotted as mean ± SEM (n = 3). p, precursor; i, intermediate.

(B–E) Radiolabeled Pam18 (B, D, and E) or Atp2 (C) were imported into the indicated mitochondria as described in Figures 1D–1F. *ssc1-3* mitochondria (B and C) were subjected to heat shock prior to the import reaction. The amounts of Proteinase K-resistant mature protein were quantified and plotted over time. Data are plotted as mean ± SEM (n = 3). m, mature.

See also Figure S3.

segments into the matrix and contribute to efficient mitochondrial biogenesis.

Tim50^{Mx} and Tim50^{TM} Promote Pam17 Function and Import Motor Activity

Because import of mature Atp2 polypeptide segments requires not only PAM activity but also a high mitochondrial Δψ, and is therefore particularly dependent on Pam17 (Gambill et al., 1993; Frazier et al., 2004; van der Laan et al., 2005; Schendzielorz et al., 2017), we explored whether any of these functions were affected by the Tim50 truncations. First, we investigated the import-driving activity exerted by the PAM machinery on a polypeptide segment accumulated at mitochondrial import sites (Figure 2A, cartoon). To this end, a chimeric preprotein consisting of the matrix-targeting element of the Cyb2 presequence fused to the passenger protein dihydrofolate reductase (DHFR), termed $b_2(167)_\Delta$DHFR (Koll et al., 1992; Voos et al., 1993), was stalled at the TOM-TIM23 import sites (Figure 2A, first incubation). The N-terminal Cyb2 matrix-targeted presequence is efficiently translocated by both the TOM and TIM23 complexes and cleaved off by MPP leading to the generation of the intermediate form of the protein, termed i-$b_2(167)_\Delta$DHFR. At the C terminus of the fusion protein, the DHFR moiety binds methotrexate, which stabilizes folding and prevents this portion of the fusion protein from passing through the TOM complex (Figure 2A, cartoon). As a result, the i-$b_2(167)_\Delta$DHFR accumulates in a two-membrane-spanning conformation (Dekker et al., 1997; Chacinska et al., 2003, 2010). The Δψ across the inner membrane can be then dissipated with the potassium-specific ionophore valinomycin to abolish the Δψ component of the inward-directed import-driving force and allow an unbiased assessment of PAM functionality (Figure 2A, second incubation) (Voisine et al., 1999; Frazier et al., 2004; Ieva et al., 2014; Schendzielorz et al., 2017). In wild-type mitochondria, the import-driving activity of PAM constrains the folded DHFR

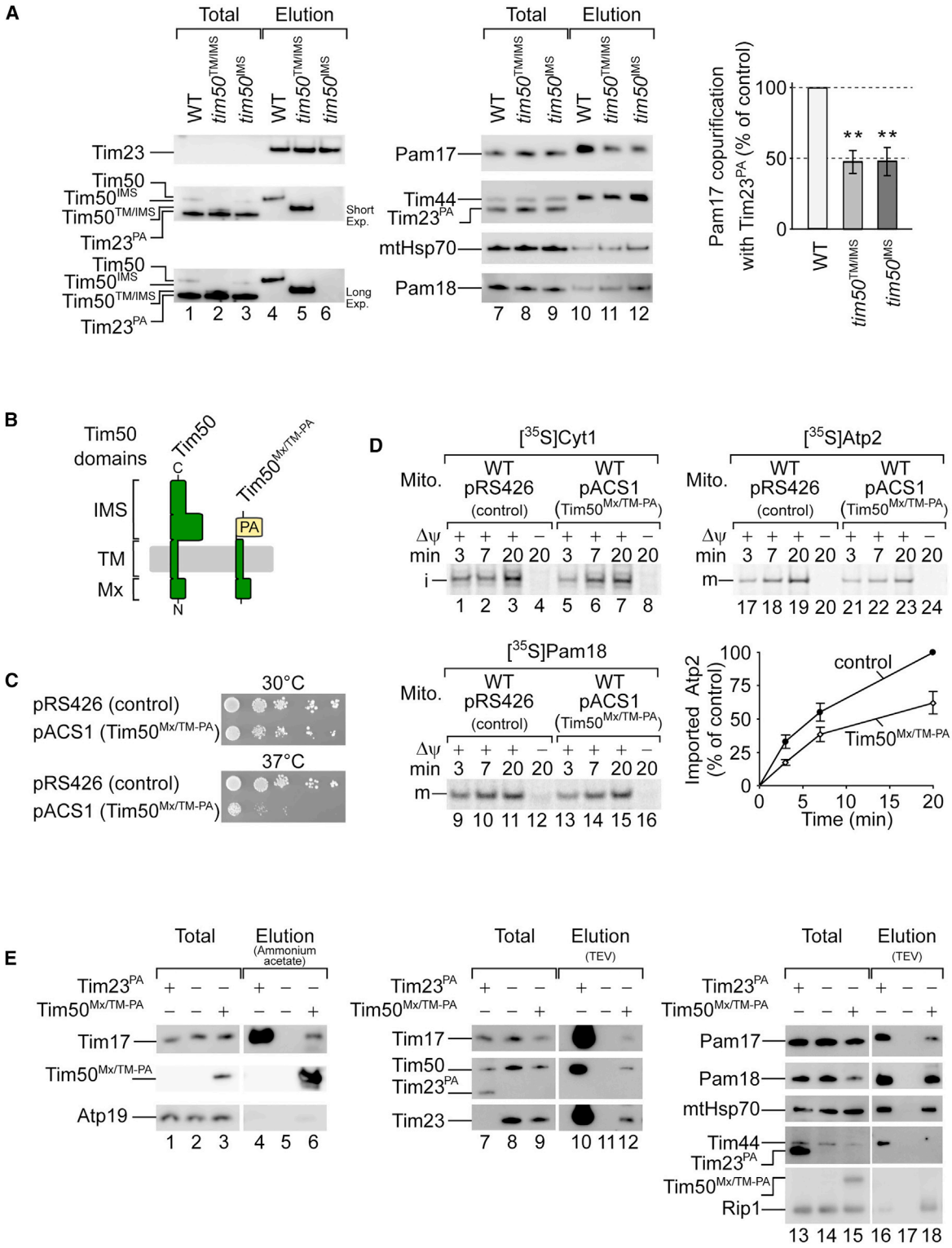

Figure 3. Distinct Roles of Tim50^{Mx} and Tim50^{TM} in Modulating TIM23-PAM Interactions

(A) Protein A-tagged Tim23 mitochondria harboring wild-type or the indicated Tim50 mutant forms were solubilized with digitonin and subjected to IgG affinity purification. Total and elution fractions were analyzed using SDS-PAGE and immunoblotting. Total, 2.5%; elution, 100%. The signals of proteins co-eluted with tagged Tim23 (bait protein) were quantified and normalized to the relative amount of the bait protein in each sample. Data are represented as mean ± SEM (n = 5). A one-tailed t test for unequal variances was performed: **p ≤ 0.01.

(legend continued on next page)

moiety proximal to the TOM complex, thus restricting its accessibility to externally added Proteinase K. The import-driving activity exerted by the PAM machinery can be inferred from the fraction of i-b_2(167)$_\Delta$DHFR that resists proteolysis. With *tim50*$^{TM/IMS}$ mitochondria, less i-b_2(167)$_\Delta$DHFR was generated during the first incubation, yet the fraction of i-b_2(167)$_\Delta$DHFR protected from Proteinase K after the second incubation was comparable with that obtained using wild-type mitochondria (Figure 2A, lanes 1–6 and quantifications), indicating normal import-driving activity generated by PAM in the absence of the Tim50^{Mx} domain. Notably, a similar protection pattern was observed for *pam17*Δ mitochondria, which produce less i-b_2(167)$_\Delta$DHFR but have a wild-type like import motor-driving activity (Figure S3) (Schendzielorz et al., 2017). In contrast, i-b_2(167)$_\Delta$-DHFR was largely digested by Proteinase K when accumulated at the import sites of *tim50*^{IMS} mitochondria (lanes 7–9 and quantifications). We conclude that the transmembrane domain of Tim50 stimulates the import-driving activity exerted by the PAM machinery on the incoming polypeptide segments.

To investigate whether the deletions of the matrix and transmembrane Tim50 domains impair the function of Pam17, we set out to identify a model protein the import of which strongly depends on Pam17, but not on import motor function. We found that the J-protein of the PAM machinery, Pam18, fulfills this criterion. Pam18 contains a single transmembrane segment exposing a small N-terminal domain to the IMS and the functionally critical J-domain to the matrix. This protein is imported by means of an atypical mitochondrial targeting signal that was reported to consist of its transmembrane segment and a C-terminally adjacent positively charged amphipathic helix (Mokranjac et al., 2007). First we asked to what extent import of Pam18 requires import motor activity. To this end, we used mitochondria harboring a temperature-sensitive mutant form of mtHsp70 that is encoded by the *ssc1-3* allele (Gambill et al., 1993). Upon heat shock, import of radiolabeled Pam18 in *ssc1-3* mitochondria was only partially affected (Figure 2B), whereas import of Atp2 in these mutant mitochondria was fully abolished (Figure 2C). In contrast to the mild effect observed upon mtHsp70 inactivation, import of Pam18 into *pam17*Δ mitochondria was strongly impaired (Figure 2D) (Schendzielorz et al., 2017), indicating that Pam17 plays a critical role during import of Pam18. Therefore, we used import of this model protein as a proxy for Pam17 functions in *tim50*-mutant mitochondria. Import of Pam18 into *tim50*$^{TM/IMS}$ mitochondria was reduced by more than half compared with import into wild-type mitochondria (Figure 2E, lanes 5–8). This defect was more severe than that observed for the import of the same model protein in *ssc1-3* mitochondria (Figure 2B), suggesting that the Pam17 function is specifically impaired in mitochondria lacking the Tim50^{Mx} domain. The additional deletion of Tim50^{TM} in *tim50*^{IMS} mitochondria worsened import of Pam18 (Figure 2E, lanes 9–12), probably accounting for the contribution of PAM activity to efficient import of this model protein. Taken together, our results show that Tim50^{Mx} specifically promotes Pam17 function, whereas Tim50^{TM} is linked to the subsequent steps of import-driving force generation by the PAM machinery.

The N-Terminal Moiety of Tim50 Interacts with Translocase-free Pam18 and Hsp70

Next we asked whether the N-terminal parts of Tim50 influence the recruitment of distinct PAM subunits to the TIM23 complex. We performed native affinity purification of the translocase harboring wild-type or N-terminally truncated forms of Tim50. Wild-type Tim50 and Tim50$^{TM/IMS}$ were efficiently co-isolated with protein A-tagged and digitonin-solubilized Tim23 (Figure 3A, lanes 4 and 5). Tim50^{IMS} was not detected in the elution fraction (Figure 3A, lane 6). Because expression of truncated Tim50^{IMS} supports cell growth under permissive conditions (Figure 1B) (Mokranjac et al., 2009) and does not substantially affect the mitochondrial $\Delta\psi$ (Figure 1C), we infer that Tim50^{IMS} does productively interact with Tim23 in intact mitochondria, but this interaction is not stable upon detergent solubilization (Malhotra et al., 2017). Pam17 was inefficiently co-eluted with tagged Tim23 in mitochondria harboring Tim50$^{TM/IMS}$ (Figure 3A, lane 11 and quantifications), whereas other PAM components, like mtHsp70, Pam18 and Tim44, were recovered in the elution fraction with wild-type like efficiency. Additional lack of the Tim50 transmembrane segment in *tim50*^{IMS} mitochondria did not further enhance the Pam17 recruitment defect observed in *tim50*$^{TM/IMS}$ mitochondria (Figure 3A, lane 12 and quantifications). Despite the strong impairment of the PAM activity (Figure 2A), Pam18, Tim44, and Hsp70 were co-isolated from *tim50*^{IMS} mitochondria with a particularly high efficiency, supporting a regulatory role of Tim50^{TM} in motor organization and cycling at the TIM23 complex (Figure 3A, lane 12) (Schulz and Rehling, 2014). Therefore, the loss of PAM-mediated import-driving force in *tim50*^{IMS} mitochondria cannot be explained by a defective physical interaction between TIM23 and PAM, but it appears to relate to the functional cooperation of the channel and import motor modules. The impaired association of Pam17 with the TIM23 complex in mitochondria lacking the N-terminal portion of Tim50 is likely to be a major cause of the import defect of Pam17-dependent preproteins, like Pam18 (Figure 2E).

To gain further insights into the role of the Tim50^{Mx} and Tim50^{TM} domains in preprotein import, we generated a fusion protein (Tim50$^{Mx/TM-PA}$) in which the C-terminal IMS domain of

(B) Schematic representation of the Tim50$^{Mx/TM-PA}$ construct. PA, protein A tag.
(C) YPH499 strains transformed either with the empty vector pRS426 (Christianson et al., 1992) or the pACS1 plasmid (encoding Tim50$^{Mx/TM-PA}$) were serially diluted and spotted onto synthetic defined media containing 2% dextrose and incubated at 30°C or 37°C.
(D) Radiolabeled preproteins were imported into the indicated mitochondria as described in Figures 1D–1F. Data are plotted as mean ± SEM (n = 3). i, intermediate; m, mature.
(E) Wild-type mitochondria or mitochondria harboring a protein A tag fused either to Tim23 or to Tim50$^{Mx/TM}$ were solubilized with digitonin and subjected to IgG affinity purification. Bound proteins were eluted using either ammonium acetate or cleavage of the protein A tag by digestion with TEV protease. Total and elution fractions were analyzed using SDS-PAGE and immunoblotting. Tim50$^{Mx/TM-PA}$ was detected using peroxidase anti-peroxidase antibodies. Total, 2.5%; elution, 100%.
See also Figure S4.

Tim50 was replaced by a protein A affinity tag (Figures 3B and S4A). We expressed this construct from a multi-copy plasmid in a wild-type strain containing the endogenous *TIM50* gene. Surprisingly, expression of $Tim50^{Mx/TM-PA}$ impaired yeast growth at 37°C (but not at 30°C), thus revealing a partial dominant-negative phenotype under these conditions (Figure 3C). Mitochondria isolated from cells expressing $Tim50^{Mx/TM-PA}$ grown under permissive conditions had a wild-type-like $\Delta\psi$, indicating that the presence of $Tim50^{Mx/TM-PA}$ does not interfere with the channel-gating function of the endogenous Tim50 protein (Figure S4B). Mitochondria containing $Tim50^{Mx/TM-PA}$ were subjected to import of differentially targeted preproteins. The PAM-independent inner-membrane-sorted preprotein Cyt1 (Figure 3D, lanes 1–8) and Pam18 (Figure 3D, lanes 9–16) were efficiently imported. In contrast, import of PAM-dependent Atp2 was partially impaired (Figure 3D, lanes 17–24 and quantifications), suggesting that expression of $Tim50^{Mx/TM-PA}$ interferes with the activity of the import motor. Mitochondria harboring a protein A tag fused to either $Tim50^{Mx/TM}$ or, for comparison, Tim23 were solubilized with digitonin and subjected to IgG affinity purification. Because our Tim50-specific antiserum recognizes only the $Tim50^{IMS}$ domain, IgG-bound proteins were eluted using ammonium acetate to allow immuno-detection of the $Tim50^{Mx/TM-PA}$ bait protein (Figure 3E, lanes 4–6) or by proteolytic cleavage of the protein A tag (lanes 10–12 and 16–18). Only small amounts of TIM23 core subunits were co-eluted with $Tim50^{Mx/TM-PA}$ (Figure 3E, lane 12). The inefficient co-isolation of the TIM23 core subunits was expected, as the IMS domain of Tim50 is important for the interaction with Tim23 (Alder et al., 2008; Tamura et al., 2009; Qian et al., 2011; Malhotra et al., 2017; Dayan et al., 2019). We conclude that most of $Tim50^{Mx/TM-PA}$ is not assembled with the core of the TIM23 complex and is therefore translocase-free. Pam17 co-eluted to some extent with $Tim50^{Mx/TM}$ (Figure 3E, lane 18). Intriguingly, however, Pam18 and mtHsp70 were efficiently co-eluted with both protein A-tagged $Tim50^{Mx/TM}$ and Tim23. The Tim44 subunit that docks mtHsp70 to the TIM23 complex was not co-isolated with tagged $Tim50^{Mx/TM}$ (Figure 3E, lane 18). Thus, protein A-tagged $Tim50^{Mx/TM}$ associates with Pam18 and mtHsp70 in the absence of the translocase core complex and of the PAM organizing subunit Tim44. These observations led us to the hypothesis that the $Tim50^{Mx/TM}$ interacts with a translocase-free pool of the chaperone/co-chaperone module Hsp70/Pam18. A distinct fraction of the Pam18 was previously found associated with respiratory chain complexes independently of TIM23 (Wiedemann et al., 2007). It has been proposed that this fraction contributes to switches between the PAM-independent inner membrane sorting state of TIM23 and the stepwise assembly of the TIM23/PAM machinery for matrix import (Wiedemann et al., 2007; Dudek et al., 2013). The notion that $Tim50^{Mx/TM}$ may interact with this respiratory chain bound pool of Pam18 is supported by the co-isolation of the cytochrome bc_1 complex subunit Rip1 with $Tim50^{Mx/TM-PA}$ (Figure 3E, lane 18). As expected, Rip1 was also co-eluted with tagged Tim23 (Figure 3E, lane 16), because the presequence translocase associates with respiratory chain complexes and this local coupling facilitates the $\Delta\psi$-dependent step of the inner membrane sorting reaction (van der Laan et al., 2006). We suggest that a molecular crosstalk between the N-terminal region of Tim50 and TIM23-free Pam18/Hsp70 may influence import motor assembly and/or its reaction cycle (Chacinska et al., 2005; Wiedemann et al., 2007; Popov-Celeketić et al., 2008; Schulz and Rehling, 2014; Schendzielorz et al., 2018).

$Tim50^{IMS}$ Promotes a Step of Motor Assembly Subsequent to Pam17 Recruitment

Finally, we asked whether $Tim50^{IMS}$ cooperates with the Tim50 N-terminal moiety in promoting motor activity, thereby exerting a function that is downstream of presequence-induced gating of the TIM23 channel. To this end, we screened a collection of conditional temperature-sensitive *tim50* mutant strains for allele variants that cause import defects not ascribable to impaired presequence recognition or to TIM23 channel gating. The allele *tim50-7* was selected on the basis of the following criteria: (1) conditional growth at temperatures lower than 37°C (Figure 4A), (2) mutations mapping solely in the IMS domain (Figure 4B), and (3) wild-type-like membrane potential (Figure 4C). In addition, the *tim50-7* mutations affect neither the steady-state levels of mitochondrial proteins (Figure S5A) nor the $\Delta\psi$-dependent import of AAC into isolated mitochondria via the TIM22 complex (Figure S5B), indicating the absence of major pleiotropic effects on mitochondrial biogenesis under permissive growth conditions. Heat shock of isolated mitochondria, however, partially inactivated the Tim50-7 variant, leading to uncoupling of the mitochondrial $\Delta\psi$ (Figure S5C). Thus, all further analyses were conducted without subjecting mitochondria to heat shock.

Import of Cyt1 into wild-type and *tim50-7* mitochondria occurred at similar rates (Figure S6A), indicating that the IMS domain of Tim50-7 does fulfill its presequence receptor function. In contrast, import of Atp2 was strongly defective (Figure S6B), suggesting that Tim50-7 specifically interferes with preprotein import into the matrix. We then imported chimeric Cyb2-DHFR model preproteins, which differentially depend on the import motor. First we tested import of $b_2(167)_\Delta$-DHFR, which is matrix targeted and requires the import-driving activity of PAM (Voos et al., 1993; Frazier et al., 2004). Import of this construct into *tim50-7* mitochondria was strongly affected (Figure 4D). The related chimeric construct $b_2(167)$-DHFR is similar in length but differs for the additional presence of the active inner membrane-sorting signal of Cyb2. This fusion protein, which is sorted into the inner membrane by TIM23 and processed twice, is less dependent on import motor activity (Voos et al., 1993; Truscott et al., 2003). Compared with the matrix-translocated $b_2(167)_\Delta$-DHFR, import of the inner membrane-sorted $b_2(167)$-DHFR into *tim50-7* mitochondria was clearly less defective (Figure 4E). The chimeric construct $b_2(220)$-DHFR contains the entire bipartite presequence and a longer segment of the mature domain of Cyb2, including the heme-binding domain. Unfolding of the heme-binding domain during import requires PAM activity (Voos et al., 1993). In line with the results obtained for the import of other PAM-dependent preproteins, Atp2 and $b_2(167)_\Delta$-DHFR, import of $b_2(220)$-DHFR was substantially defective in *tim50-7* mitochondria (Figure 4F). We conclude that the extent of import defect for a series of well-characterized and related model preproteins in *tim50-7* mutant mitochondria correlates with their degree of import motor dependence. We cannot, however, fully rule

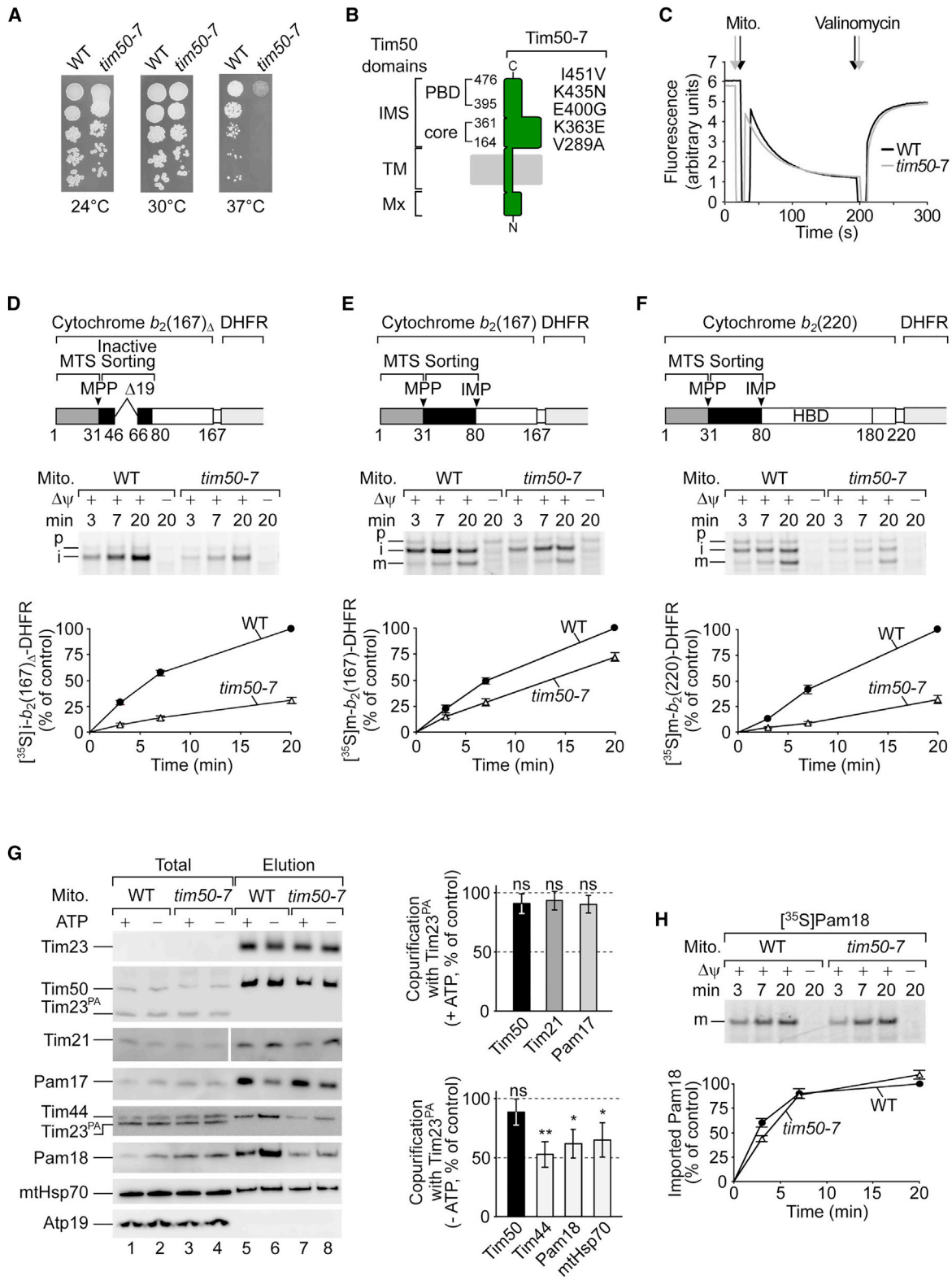

Figure 4. Expression of *tim50-7* Impairs Import Motor Assembly at a Stage Subsequent to Pam17 Recruitment to TIM23

(A) Serial dilutions of wild-type and *tim50-7* strains. Diluted cells were spotted onto YPD plates and incubated at the indicated temperatures.

(B) Schematic representation of Tim50 domains and list of amino acid substitutions encoded by the *tim50-7* allele.

(legend continued on next page)

out minor effects of the *tim50-7* mutations on PAM-independent inner membrane sorting of preproteins.

We aimed to obtain more insight into the molecular basis for the reduced efficiency of PAM-dependent preprotein import in *tim50-7* mitochondria. To this end, we expressed protein A-tagged Tim23 in the *tim50-7* strain and analyzed the physical coupling of TIM23 and PAM by IgG affinity purification from digitonin extracts of isolated mitochondria. Because ATP levels influence motor organization (Rassow et al., 1994; Schneider et al., 1994; von Ahsen et al., 1995; Liu et al., 2003; Miyata et al., 2017), mitochondria were supplied with or depleted of ATP prior to affinity purification. The amounts of Tim50 that co-purified with Tim23 were comparable with mitochondria harboring either wild-type Tim50 or Tim50-7 (Figure 4G). Likewise, Tim21, which associates with the PAM-independent inner membrane sorting form of TIM23, and Pam17 were co-eluted with similar efficiency. In contrast, the amounts of co-eluted Tim44 and Pam18 were reduced by almost half with *tim50-7* mitochondria, independently of ATP supply. The amount of co-eluted mtHsp70 was also reduced, although to a slightly lower extent. We conclude that expression of the *tim50-7* allele does not interfere with the association of Pam17 with TIM23 but impairs the subsequent stepwise recruitment of essential import motor subunits. The functionality of Pam17 at the TIM23 complex was further confirmed by the observation that the Pam17-dependent Pam18 protein was efficiently imported into isolated *tim50-7* mitochondria (Figure 4H). We therefore infer that the import defect observed in *tim50-7* mitochondria is caused by a defect in the dynamic assembly of the import motor at preprotein import sites downstream of the Pam17-mediated functions.

DISCUSSION

How the receptor, channel, and motor functions of the TIM23/PAM machinery are coordinated to achieve accurate and efficient preprotein import at the inner membrane is a major open question in mitochondrial biogenesis. Previous models inherently implied that the molecular nature of the preprotein segment within the protein-conducting channel triggers dynamic switches in the assembly and activity state of the TIM23 complex (Chacinska et al., 2005, 2010; Popov-Celeketić et al., 2008; Endo and Yamano, 2009; Mokranjac and Neupert, 2010; van der Laan et al., 2010; Schulz et al., 2015). However, there is emerging evidence that structural and functional changes in the TIM23 complex and PAM machinery may already be triggered upon preprotein binding to the TIM23 receptor domain on the IMS side of the inner membrane (Tamura et al., 2009; Schulz et al., 2011; Lytovchenko et al., 2013; Schendzielorz et al., 2017). The molecular requirements for such information transfer across the inner membrane have been unknown. We have used a combination of domain dissection and conditional mutant analysis to elucidate the role of Tim50 after presequence-mediated gating of the TIM23 channel by $Tim50^{IMS}$ (Figure 5, step 1). We show that the matrix domain of Tim50 is a critical determinant for the TIM23-Pam17 association (Figure 5, step 2). Once recruited to the channel module, Pam17 can then contribute to prime translocation into the matrix of polypeptide segments downstream of the presequence (van der Laan et al., 2005; Popov-Celeketić et al., 2008; Schiller, 2009; Lytovchenko et al., 2013; Schendzielorz et al., 2017). Our results further reveal that the subsequent stepwise association of the import motor with TIM23 is initiated by the C-terminal IMS domain of Tim50 (Figure 5, step 3). Amino acid substitutions that map solely in the IMS domain of the Tim50-7 variant described here lead to an import motor assembly defect downstream of the Pam17 recruitment step. Notably, these amino acid substitutions in $Tim50^{IMS}$ mimic specific mutations in Tim44, the matrix-localized organizer of the PAM complex, that cause a PAM assembly defect independent of Pam17 recruitment (Hutu et al., 2008). We show that the transmembrane segment of Tim50 is not required for PAM recruitment to TIM23 but supports the generation of an inward-directed driving force on the preprotein by the import motor (Figure 5, step 4). When the PAM machinery starts to pull on the N-terminal portions of a matrix-destined polypeptide segment, its C-terminal regions may still interact with the Tim50 receptor domain on the IMS site. It would be conceivable that this preprotein-Tim50 interaction determines the follow-up assembly and functional state of the PAM machinery at the *trans* site of the inner membrane. Interactions between the $Tim50^{IMS}$ domain with the channel-forming Tim23 subunit have been previously proposed to influence channel and import motor activities (Tamura et al., 2009; Lytovchenko et al., 2013; Malhotra et al., 2017; Dayan et al., 2019). On the basis of our findings, the Tim50 membrane anchor emerges as an important functional link coupling the receptor and the motor modules of the TIM23-PAM complex, which are on opposite sides of the inner membrane. In the

(C) Measurement of the membrane potential with isolated wild-type and *tim50-7* mitochondria as described in Figure 1C.

(D–F) Top: schematic representation of the Cyb2-DHFR chimeric model preproteins. MTS, matrix-targeting sequence; MPP, mitochondrial processing peptidase; IMP, inner membrane protease; HBD, heme-binding domain. Bottom: radiolabeled preproteins were imported for different periods of time into wild-type and *tim50-7* mitochondria and analyzed as in Figures 1D–1F. The amounts of the matrix-targeted i-$b_2(167)_\Delta$-DHFR (D) or inner membrane-targeted m-$b_2(167)$-DHFR (E) and m-$b_2(220)$-DHFR (F) proteins were quantified. Data are plotted as mean ± SEM ($n \geq 3$). p, precursor; i, intermediate; m, mature.

(G) Mitochondria harboring a protein A tag N-terminally fused to Tim23 ($Tim23^{PA}$) and either wild-type Tim50 or the mutant form Tim50-7 protein variant were subjected to ATP depletion. ATP was subsequently supplemented or not as indicated. Mitochondria were solubilized with digitonin and subjected to IgG affinity purification. Total and elution fractions were analyzed using SDS-PAGE and immunoblotting using the indicated antisera. Total, 2.5%; elution, 100%. The amounts of signals of the indicated Tim23 co-eluted proteins were quantified and normalized for the amount of eluted Tim23 in the same sample. Quantifications of co-eluted PAM proteins are reported for the condition that favored interaction stability (+ATP in the case of Pam17 and −ATP in the case of Tim44, Pam18, and Hsp70). Tim50 and Tim21 were quantified for the +ATP condition. Data are represented as mean ± SEM ($n \geq 3$). A one-tailed t test for unequal variances was performed: *$p \leq 0.05$ and **$p \leq 0.01$; ns, non-significant ($p \geq 0.05$).

(H) Radiolabeled Pam18 was imported into wild-type and *tim50-7* mitochondria and analyzed as in Figures 1D–1F. Plotted data correspond to mean value ± SEM ($n = 3$).

See also Figures S5 and S6.

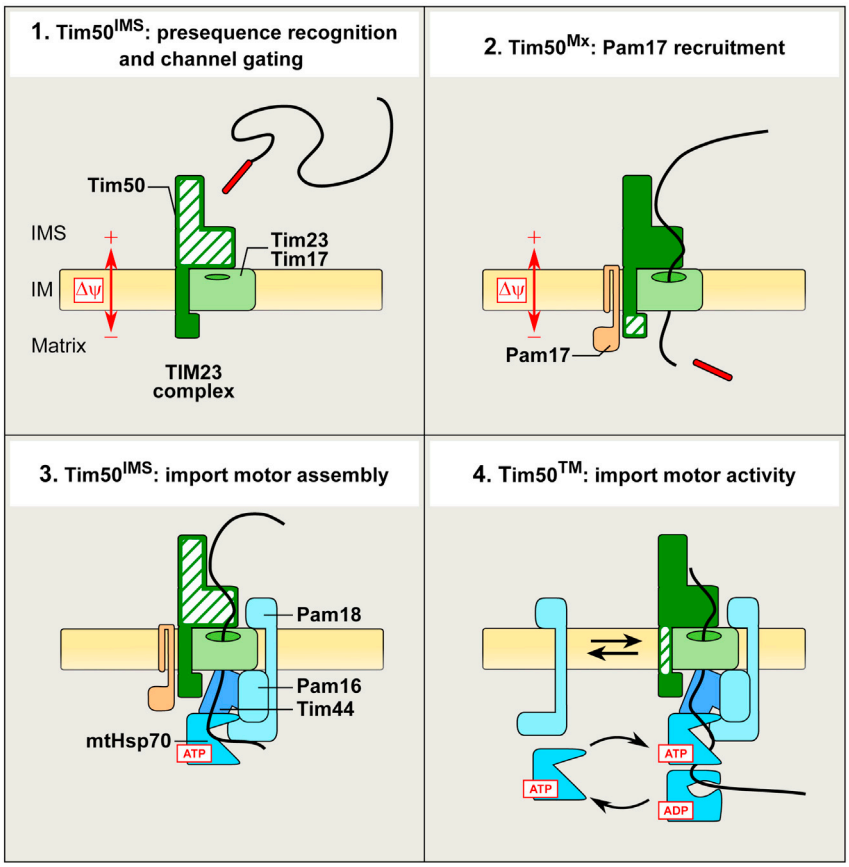

Figure 5. Schematic Representation of the Roles of Tim50 during Preprotein Import

Step 1: the IMS domain of Tim50 controls the opening of the TIM23 channel. Recognition of a presequence signal by Tim50 induces channel gating, initiating the $\Delta\psi$-dependent transport of the presequence by TIM23. Step 2: the matrix domain of Tim50 is a critical determinant for the TIM23-Pam17 association. Pam17 in turn facilitates further $\Delta\psi$-dependent transport steps downstream of presequence translocation. Step 3: the IMS domain of Tim50 licenses the subsequent stepwise association of the import motor subunits with TIM23. Step 4: the transmembrane segment of Tim50 stimulates the generation of an inward-directed driving force on the preprotein by the import motor. For clarity, only the essential core subunits of the TIM23 complex and the PAM subunits are represented. The Tim50 domains promoting each of the described steps are highlighted with green stripe patterns.

case of inner membrane-targeted preproteins, the incoming polypeptide containing a stop-transfer signal may occupy a position of the TIM23 channel with a facilitated access to the external lipid bilayer rather than to the pulling activity of the import motor (Popov-Celeketić et al., 2008; Chacinska et al., 2010; Ieva et al., 2014; Schendzielorz et al., 2018). Thus, mutations in Tim50 or its depletion may have marginal effects on inner membrane targeting of preproteins that have small matrix domains and do not strictly require PAM activity. However, the coordination of the Tim50 IMS receptor function with the PAM assembly and functional state may be particularly important for the import of preproteins that contain both motor-dependent matrix domains and inner membrane-integral domains. The complex biogenesis of such preproteins is likely to require multiple switches within the import machinery that involve the cycling of PAM subunits, such as Pam18 and mtHsp70 (Liu et al., 2003; D'Silva et al., 2004; Bohnert et al., 2010; Schulz and Rehling, 2014).

Taken together, we propose that dynamic rearrangements in the IMS domain of the Tim50 receptor, most likely induced by the interaction with the preprotein polypeptide segments, trigger the assembly and activation of the import motor on the matrix side of the TIM23 preprotein-conducting channel. Our data support a model in which Tim50 plays a key role in the orchestration of the functional interplay between the TIM23 complex and PAM machinery that allows accurate discrimination of matrix-translocated polypeptide segments.

STAR★METHODS

Detailed methods are provided in the online version of this paper and include the following:

- KEY RESOURCES TABLE
- LEAD CONTACT AND MATERIALS AVAILABILITY
- EXPERIMENTAL MODEL AND SUBJECT DETAILS
- METHOD DETAILS
  - Yeast Strains, Plasmids and Growth Conditions
  - Mitochondria Isolation, Analysis of Protein Content and Mitochondrial $\Delta\psi$ Measurement
  - *In Vitro* Preprotein Synthesis and Import into Isolated Mitochondria
  - Native Isolation of Protein Complexes by IgG Affinity Purification
- QUANTIFICATION AND STATISTICAL ANALYSIS
- DATA AND CODE AVAILABILITY

SUPPLEMENTAL INFORMATION

Supplemental Information can be found online at https://doi.org/10.1016/j.celrep.2020.02.031.

ACKNOWLEDGMENTS

We thank Klaus Pfanner (University of Freiburg, Germany) for discussion. This work was supported by a PhD fellowship of the French Ligue Contre Le Cancer to C.M., funding from Deutsche Forschungsgemeinschaft (IRTG 1830, SFB746, and SFB 894, Germany) to M.v.d.L., and the French CNRS ATIP program to R.I.

AUTHOR CONTRIBUTIONS

R.I. and M.v.d.L. conceived and designed the research and supervised the project. R.I., A.C.-S., C.M., L.P., and B.G. performed the experiments. R.I. and M.v.d.L. wrote the manuscript with contributions from A.C.-S. A.C.-S. and C.M. prepared the figures. All authors analyzed the data, discussed the experimental results, and commented on the manuscript.

DECLARATION OF INTERESTS

The authors declare no competing interests.

Received: September 29, 2019
Revised: December 13, 2019
Accepted: February 7, 2020
Published: March 3, 2020

REFERENCES

Alder, N.N., Sutherland, J., Buhring, A.I., Jensen, R.E., and Johnson, A.E. (2008). Quaternary structure of the mitochondrial TIM23 complex reveals dynamic association between Tim23p and other subunits. Mol. Biol. Cell *19*, 159–170.

Banerjee, R., Gladkova, C., Mapa, K., Witte, G., and Mokranjac, D. (2015). Protein translocation channel of mitochondrial inner membrane and matrix-exposed import motor communicate via two-domain coupling protein. eLife *4*, e11897.

Blom, J., Kübrich, M., Rassow, J., Voos, W., Dekker, P.J., Maarse, A.C., Meijer, M., and Pfanner, N. (1993). The essential yeast protein MIM44 (encoded by MPI1) is involved in an early step of preprotein translocation across the mitochondrial inner membrane. Mol. Cell. Biol. *13*, 7364–7371.

Bohnert, M., Rehling, P., Guiard, B., Herrmann, J.M., Pfanner, N., and van der Laan, M. (2010). Cooperation of stop-transfer and conservative sorting mechanisms in mitochondrial protein transport. Curr. Biol. *20*, 1227–1232.

Chacinska, A., Rehling, P., Guiard, B., Frazier, A.E., Schulze-Specking, A., Pfanner, N., Voos, W., and Meisinger, C. (2003). Mitochondrial translocation contact sites: separation of dynamic and stabilizing elements in formation of a TOM-TIM-preprotein supercomplex. EMBO J. *22*, 5370–5381.

Chacinska, A., Lind, M., Frazier, A.E., Dudek, J., Meisinger, C., Geissler, A., Sickmann, A., Meyer, H.E., Truscott, K.N., Guiard, B., et al. (2005). Mitochondrial presequence translocase: switching between TOM tethering and motor recruitment involves Tim21 and Tim17. Cell *120*, 817–829.

Chacinska, A., Koehler, C.M., Milenkovic, D., Lithgow, T., and Pfanner, N. (2009). Importing mitochondrial proteins: machineries and mechanisms. Cell *138*, 628–644.

Chacinska, A., van der Laan, M., Mehnert, C.S., Guiard, B., Mick, D.U., Hutu, D.P., Truscott, K.N., Wiedemann, N., Meisinger, C., Pfanner, N., and Rehling, P. (2010). Distinct forms of mitochondrial TOM-TIM supercomplexes define signal-dependent states of preprotein sorting. Mol. Cell. Biol. *30*, 307–318.

Christianson, T.W., Sikorski, R.S., Dante, M., Shero, J.H., and Hieter, P. (1992). Multifunctional yeast high-copy-number shuttle vectors. Gene *110*, 119–122.

Craig, E.A. (2018). Hsp70 at the membrane: driving protein translocation. BMC Biol. *16*, 11.

D'Silva, P.D., Schilke, B., Walter, W., Andrew, A., and Craig, E.A. (2003). J protein cochaperone of the mitochondrial inner membrane required for protein import into the mitochondrial matrix. Proc. Natl. Acad. Sci. U S A *100*, 13839–13844.

D'Silva, P., Liu, Q., Walter, W., and Craig, E.A. (2004). Regulated interactions of mtHsp70 with Tim44 at the translocon in the mitochondrial inner membrane. Nat. Struct. Mol. Biol. *11*, 1084–1091.

D'Silva, P.R., Schilke, B., Walter, W., and Craig, E.A. (2005). Role of Pam16's degenerate J domain in protein import across the mitochondrial inner membrane. Proc. Natl. Acad. Sci. U S A *102*, 12419–12424.

Dayan, D., Bandel, M., Günsel, U., Nussbaum, I., Prag, G., Mokranjac, D., Neupert, W., and Azem, A. (2019). A mutagenesis analysis of Tim50, the major receptor of the TIM23 complex, identifies regions that affect its interaction with Tim23. Sci. Rep. *9*, 2012.

Dekker, P.J., Martin, F., Maarse, A.C., Bömer, U., Müller, H., Guiard, B., Meijer, M., Rassow, J., and Pfanner, N. (1997). The Tim core complex defines the number of mitochondrial translocation contact sites and can hold arrested preproteins in the absence of matrix Hsp70-Tim44. EMBO J. *16*, 5408–5419.

Demishtein-Zohary, K., and Azem, A. (2017). The TIM23 mitochondrial protein import complex: function and dysfunction. Cell Tissue Res. *367*, 33–41.

Dudek, J., Rehling, P., and van der Laan, M. (2013). Mitochondrial protein import: common principles and physiological networks. Biochim. Biophys. Acta *1833*, 274–285.

Endo, T., and Yamano, K. (2009). Multiple pathways for mitochondrial protein traffic. Biol. Chem. *390*, 723–730.

Filipuzzi, I., Steffen, J., Germain, M., Goepfert, L., Conti, M.A., Potting, C., Cerino, R., Pfeifer, M., Krastel, P., Hoepfner, D., et al. (2017). Stendomycin selectively inhibits TIM23-dependent mitochondrial protein import. Nat. Chem. Biol. *13*, 1239–1244.

Frazier, A.E., Dudek, J., Guiard, B., Voos, W., Li, Y., Lind, M., Meisinger, C., Geissler, A., Sickmann, A., Meyer, H.E., et al. (2004). Pam16 has an essential role in the mitochondrial protein import motor. Nat. Struct. Mol. Biol. *11*, 226–233.

Gambill, B.D., Voos, W., Kang, P.J., Miao, B., Langer, T., Craig, E.A., and Pfanner, N. (1993). A dual role for mitochondrial heat shock protein 70 in membrane translocation of preproteins. J. Cell Biol. *123*, 109–117.

Gebert, M., Schrempp, S.G., Mehnert, C.S., Heisswolf, A.K., Oeljeklaus, S., Ieva, R., Bohnert, M., von der Malsburg, K., Wiese, S., Kleinschroth, T., et al. (2012). Mgr2 promotes coupling of the mitochondrial presequence translocase to partner complexes. J. Cell Biol. *197*, 595–604.

Geissler, A., Chacinska, A., Truscott, K.N., Wiedemann, N., Brandner, K., Sickmann, A., Meyer, H.E., Meisinger, C., Pfanner, N., and Rehling, P. (2002). The mitochondrial presequence translocase: an essential role of Tim50 in directing preproteins to the import channel. Cell *111*, 507–518.

Glick, B.S., Brandt, A., Cunningham, K., Müller, S., Hallberg, R.L., and Schatz, G. (1992). Cytochromes c1 and b2 are sorted to the intermembrane space of yeast mitochondria by a stop-transfer mechanism. Cell *69*, 809–822.

Hansen, K.G., and Herrmann, J.M. (2019). Transport of proteins into mitochondria. Protein J. *38*, 330–342.

Horst, M., Jenö, P., Kronidou, N.G., Bolliger, L., Oppliger, W., Scherer, P., Manning-Krieg, U., Jascur, T., and Schatz, G. (1993). Protein import into yeast mitochondria: the inner membrane import site protein ISP45 is the MPI1 gene product. EMBO J. *12*, 3035–3041.

Hutu, D.P., Guiard, B., Chacinska, A., Becker, D., Pfanner, N., Rehling, P., and van der Laan, M. (2008). Mitochondrial protein import motor: differential role of Tim44 in the recruitment of Pam17 and J-complex to the presequence translocase. Mol. Biol. Cell *19*, 2642–2649.

Ieva, R., Schrempp, S.G., Opaliński, L., Wollweber, F., Höß, P., Heißwolf, A.K., Gebert, M., Zhang, Y., Guiard, B., Rospert, S., et al. (2014). Mgr2 functions as lateral gatekeeper for preprotein sorting in the mitochondrial inner membrane. Mol. Cell *56*, 641–652.

Kang, Y., Fielden, L.F., and Stojanovski, D. (2018). Mitochondrial protein transport in health and disease. Semin. Cell Dev. Biol. *76*, 142–153.

Koll, H., Guiard, B., Rassow, J., Ostermann, J., Horwich, A.L., Neupert, W., and Hartl, F.U. (1992). Antifolding activity of hsp60 couples protein import into the mitochondrial matrix with export to the intermembrane space. Cell *68*, 1163–1175.

Kozany, C., Mokranjac, D., Sichting, M., Neupert, W., and Hell, K. (2004). The J domain-related cochaperone Tim16 is a constituent of the mitochondrial TIM23 preprotein translocase. Nat. Struct. Mol. Biol. *11*, 234–241.

Liu, Q., D'Silva, P., Walter, W., Marszalek, J., and Craig, E.A. (2003). Regulated cycling of mitochondrial Hsp70 at the protein import channel. Science *300*, 139–141.

Lytovchenko, O., Melin, J., Schulz, C., Kilisch, M., Hutu, D.P., and Rehling, P. (2013). Signal recognition initiates reorganization of the presequence translocase during protein import. EMBO J. *32*, 886–898.

Malhotra, K., Modak, A., Nangia, S., Daman, T.H., Gunsel, U., Robinson, V.L., Mokranjac, D., May, E.R., and Alder, N.N. (2017). Cardiolipin mediates membrane and channel interactions of the mitochondrial TIM23 protein import complex receptor Tim50. Sci. Adv. *3*, e1700532.

Marom, M., Azem, A., and Mokranjac, D. (2011). Understanding the molecular mechanism of protein translocation across the mitochondrial inner membrane: still a long way to go. Biochim. Biophys. Acta *1808*, 990–1001.

Martin, J., Mahlke, K., and Pfanner, N. (1991). Role of an energized inner membrane in mitochondrial protein import. Delta psi drives the movement of presequences. J. Biol. Chem. *266*, 18051–18057.

Martinez-Caballero, S., Grigoriev, S.M., Herrmann, J.M., Campo, M.L., and Kinnally, K.W. (2007). Tim17p regulates the twin pore structure and voltage gating of the mitochondrial protein import complex TIM23. J. Biol. Chem. *282*, 3584–3593.

Matta, S.K., Pareek, G., Bankapalli, K., Oblesha, A., and D'Silva, P. (2017). Role of Tim17 transmembrane regions in regulating the architecture of presequence translocase and mitochondrial DNA stability. Mol. Cell. Biol. *37*, e00491.

Meinecke, M., Wagner, R., Kovermann, P., Guiard, B., Mick, D.U., Hutu, D.P., Voos, W., Truscott, K.N., Chacinska, A., Pfanner, N., and Rehling, P. (2006). Tim50 maintains the permeability barrier of the mitochondrial inner membrane. Science *312*, 1523–1526.

Meisinger, C., Pfanner, N., and Truscott, K.N. (2006). Isolation of yeast mitochondria. Methods Mol. Biol. *313*, 33–39.

Milisav, I., Moro, F., Neupert, W., and Brunner, M. (2001). Modular structure of the TIM23 preprotein translocase of mitochondria. J. Biol. Chem. *276*, 25856–25861.

Miyata, N., Tang, Z., Conti, M.A., Johnson, M.E., Douglas, C.J., Hasson, S.A., Damoiseaux, R., Chang, C.A., and Koehler, C.M. (2017). Adaptation of a genetic screen reveals an inhibitor for mitochondrial protein import component Tim44. J. Biol. Chem. *292*, 5429–5442.

Mokranjac, D., and Neupert, W. (2009). Thirty years of protein translocation into mitochondria: unexpectedly complex and still puzzling. Biochim. Biophys. Acta *1793*, 33–41.

Mokranjac, D., and Neupert, W. (2010). The many faces of the mitochondrial TIM23 complex. Biochim. Biophys. Acta *1797*, 1045–1054.

Mokranjac, D., Paschen, S.A., Kozany, C., Prokisch, H., Hoppins, S.C., Nargang, F.E., Neupert, W., and Hell, K. (2003a). Tim50, a novel component of the TIM23 preprotein translocase of mitochondria. EMBO J. *22*, 816–825.

Mokranjac, D., Sichting, M., Neupert, W., and Hell, K. (2003b). Tim14, a novel key component of the import motor of the TIM23 protein translocase of mitochondria. EMBO J. *22*, 4945–4956.

Mokranjac, D., Berg, A., Adam, A., Neupert, W., and Hell, K. (2007). Association of the Tim14.Tim16 subcomplex with the TIM23 translocase is crucial for function of the mitochondrial protein import motor. J. Biol. Chem. *282*, 18037–18045.

Mokranjac, D., Sichting, M., Popov-Celeketić, D., Mapa, K., Gevorkyan-Airapetov, L., Zohary, K., Hell, K., Azem, A., and Neupert, W. (2009). Role of Tim50 in the transfer of precursor proteins from the outer to the inner membrane of mitochondria. Mol. Biol. Cell *20*, 1400–1407.

Moulin, C., Caumont-Sarcos, A., and Ieva, R. (2019). Mitochondrial presequence import: Multiple regulatory knobs fine-tune mitochondrial biogenesis and homeostasis. Biochim. Biophys. Acta Mol. Cell Res. *1866*, 930–944.

Palmisano, A., Zara, V., Hönlinger, A., Vozza, A., Dekker, P.J., Pfanner, N., and Palmieri, F. (1998). Targeting and assembly of the oxoglutarate carrier: general principles for biogenesis of carrier proteins of the mitochondrial inner membrane. Biochem. J. *333*, 151–158.

Pfanner, N., Warscheid, B., and Wiedemann, N. (2019). Mitochondrial proteins: from biogenesis to functional networks. Nat. Rev. Mol. Cell Biol. *20*, 267–284.

Popov-Celeketić, D., Mapa, K., Neupert, W., and Mokranjac, D. (2008). Active remodelling of the TIM23 complex during translocation of preproteins into mitochondria. EMBO J. *27*, 1469–1480.

Poveda-Huertes, D., Mulica, P., and Vögtle, F.N. (2017). The versatility of the mitochondrial presequence processing machinery: cleavage, quality control and turnover. Cell Tissue Res. *367*, 73–81.

Qian, X., Gebert, M., Höpker, J., Yan, M., Li, J., Wiedemann, N., van der Laan, M., Pfanner, N., and Sha, B. (2011). Structural basis for the function of Tim50 in the mitochondrial presequence translocase. J. Mol. Biol. *411*, 513–519.

Rahman, B., Kawano, S., Yunoki-Esaki, K., Anzai, T., and Endo, T. (2014). NMR analyses on the interactions of the yeast Tim50 C-terminal region with the presequence and Tim50 core domain. FEBS Lett. *588*, 678–684.

Ramesh, A., Peleh, V., Martinez-Caballero, S., Wollweber, F., Sommer, F., van der Laan, M., Schroda, M., Alexander, R.T., Campo, M.L., and Herrmann, J.M. (2016). A disulfide bond in the TIM23 complex is crucial for voltage gating and mitochondrial protein import. J. Cell Biol. *214*, 417–431.

Rassow, J., Maarse, A.C., Krainer, E., Kübrich, M., Müller, H., Meijer, M., Craig, E.A., and Pfanner, N. (1994). Mitochondrial protein import: biochemical and genetic evidence for interaction of matrix hsp70 and the inner membrane protein MIM44. J. Cell Biol. *127*, 1547–1556.

Ryan, M.T., Müller, H., and Pfanner, N. (1999). Functional staging of ADP/ATP carrier translocation across the outer mitochondrial membrane. J. Biol. Chem. *274*, 20619–20627.

Schendzielorz, A.B., Schulz, C., Lytovchenko, O., Clancy, A., Guiard, B., Ieva, R., van der Laan, M., and Rehling, P. (2017). Two distinct membrane potential-dependent steps drive mitochondrial matrix protein translocation. J. Cell Biol. *216*, 83–92.

Schendzielorz, A.B., Bragoszewski, P., Naumenko, N., Gomkale, R., Schulz, C., Guiard, B., Chacinska, A., and Rehling, P. (2018). Motor recruitment to the TIM23 channel's lateral gate restricts polypeptide release into the inner membrane. Nat. Commun. *9*, 4028.

Schiller, D. (2009). Pam17 and Tim44 act sequentially in protein import into the mitochondrial matrix. Int. J. Biochem. Cell Biol. *41*, 2343–2349.

Schneider, H.C., Berthold, J., Bauer, M.F., Dietmeier, K., Guiard, B., Brunner, M., and Neupert, W. (1994). Mitochondrial Hsp70/MIM44 complex facilitates protein import. Nature *371*, 768–774.

Schulz, C., and Rehling, P. (2014). Remodelling of the active presequence translocase drives motor-dependent mitochondrial protein translocation. Nat. Commun. *5*, 4349.

Schulz, C., Lytovchenko, O., Melin, J., Chacinska, A., Guiard, B., Neumann, P., Ficner, R., Jahn, O., Schmidt, B., and Rehling, P. (2011). Tim50's presequence receptor domain is essential for signal driven transport across the TIM23 complex. J. Cell Biol. *195*, 643–656.

Schulz, C., Schendzielorz, A., and Rehling, P. (2015). Unlocking the presequence import pathway. Trends Cell Biol. *25*, 265–275.

Shiota, T., Mabuchi, H., Tanaka-Yamano, S., Yamano, K., and Endo, T. (2011). In vivo protein-interaction mapping of a mitochondrial translocator protein Tom22 at work. Proc. Natl. Acad. Sci. U S A *108*, 15179–15183.

Sikorski, R.S., and Hieter, P. (1989). A system of shuttle vectors and yeast host strains designed for efficient manipulation of DNA in *Saccharomyces cerevisiae*. Genetics *122*, 19–27.

Tamura, Y., Harada, Y., Shiota, T., Yamano, K., Watanabe, K., Yokota, M., Yamamoto, H., Sesaki, H., and Endo, T. (2009). Tim23-Tim50 pair coordinates functions of translocators and motor proteins in mitochondrial protein import. J. Cell Biol. *184*, 129–141.

Teixeira, P.F., and Glaser, E. (2013). Processing peptidases in mitochondria and chloroplasts. Biochim. Biophys. Acta *1833*, 360–370.

Ting, S.Y., Schilke, B.A., Hayashi, M., and Craig, E.A. (2014). Architecture of the TIM23 inner mitochondrial translocon and interactions with the matrix import motor. J. Biol. Chem. *289*, 28689–28696.

Ting, S.Y., Yan, N.L., Schilke, B.A., and Craig, E.A. (2017). Dual interaction of scaffold protein Tim44 of mitochondrial import motor with channel-forming translocase subunit Tim23. eLife *6*, e23609.

Truscott, K.N., Kovermann, P., Geissler, A., Merlin, A., Meijer, M., Driessen, A.J., Rassow, J., Pfanner, N., and Wagner, R. (2001). A presequence- and voltage-sensitive channel of the mitochondrial preprotein translocase formed by Tim23. Nat. Struct. Biol. *8*, 1074–1082.

Truscott, K.N., Voos, W., Frazier, A.E., Lind, M., Li, Y., Geissler, A., Dudek, J., Müller, H., Sickmann, A., Meyer, H.E., et al. (2003). A J-protein is an essential subunit of the presequence translocase-associated protein import motor of mitochondria. J. Cell Biol. *163*, 707–713.

Turakhiya, U., von der Malsburg, K., Gold, V.A.M., Guiard, B., Chacinska, A., van der Laan, M., and Ieva, R. (2016). Protein import by the mitochondrial presequence translocase in the absence of a membrane potential. J. Mol. Biol. *428*, 1041–1052.

Ungermann, C., Neupert, W., and Cyr, D.M. (1994). The role of Hsp70 in conferring unidirectionality on protein translocation into mitochondria. Science *266*, 1250–1253.

van der Laan, M., Chacinska, A., Lind, M., Perschil, I., Sickmann, A., Meyer, H.E., Guiard, B., Meisinger, C., Pfanner, N., and Rehling, P. (2005). Pam17 is required for architecture and translocation activity of the mitochondrial protein import motor. Mol. Cell. Biol. *25*, 7449–7458.

van der Laan, M., Wiedemann, N., Mick, D.U., Guiard, B., Rehling, P., and Pfanner, N. (2006). A role for Tim21 in membrane-potential-dependent preprotein sorting in mitochondria. Curr. Biol. *16*, 2271–2276.

van der Laan, M., Meinecke, M., Dudek, J., Hutu, D.P., Lind, M., Perschil, I., Guiard, B., Wagner, R., Pfanner, N., and Rehling, P. (2007). Motor-free mitochondrial presequence translocase drives membrane integration of preproteins. Nat. Cell Biol. *9*, 1152–1159.

van der Laan, M., Hutu, D.P., and Rehling, P. (2010). On the mechanism of preprotein import by the mitochondrial presequence translocase. Biochim. Biophys. Acta *1803*, 732–739.

Vögtle, F.N., Wortelkamp, S., Zahedi, R.P., Becker, D., Leidhold, C., Gevaert, K., Kellermann, J., Voos, W., Sickmann, A., Pfanner, N., and Meisinger, C. (2009). Global analysis of the mitochondrial N-proteome identifies a processing peptidase critical for protein stability. Cell *139*, 428–439.

Voisine, C., Craig, E.A., Zufall, N., von Ahsen, O., Pfanner, N., and Voos, W. (1999). The protein import motor of mitochondria: unfolding and trapping of preproteins are distinct and separable functions of matrix Hsp70. Cell *97*, 565–574.

von Ahsen, O., Voos, W., Henninger, H., and Pfanner, N. (1995). The mitochondrial protein import machinery. Role of ATP in dissociation of the Hsp70.Mim44 complex. J. Biol. Chem. *270*, 29848–29853.

Voos, W., Gambill, B.D., Guiard, B., Pfanner, N., and Craig, E.A. (1993). Presequence and mature part of preproteins strongly influence the dependence of mitochondrial protein import on heat shock protein 70 in the matrix. J. Cell Biol. *123*, 119–126.

Voos, W., von Ahsen, O., Müller, H., Guiard, B., Rassow, J., and Pfanner, N. (1996). Differential requirement for the mitochondrial Hsp70-Tim44 complex in unfolding and translocation of preproteins. EMBO J. *15*, 2668–2677.

Waegemann, K., Popov-Čeleketić, D., Neupert, W., Azem, A., and Mokranjac, D. (2015). Cooperation of TOM and TIM23 complexes during translocation of proteins into mitochondria. J. Mol. Biol. *427*, 1075–1084.

Wenz, L.S., Opaliński, L., Schuler, M.H., Ellenrieder, L., Ieva, R., Böttinger, L., Qiu, J., van der Laan, M., Wiedemann, N., Guiard, B., et al. (2014). The presequence pathway is involved in protein sorting to the mitochondrial outer membrane. EMBO Rep. *15*, 678–685.

Wiedemann, N., van der Laan, M., Hutu, D.P., Rehling, P., and Pfanner, N. (2007). Sorting switch of mitochondrial presequence translocase involves coupling of motor module to respiratory chain. J. Cell Biol. *179*, 1115–1122.

Wrobel, L., Sokol, A.M., Chojnacka, M., and Chacinska, A. (2016). The presence of disulfide bonds reveals an evolutionarily conserved mechanism involved in mitochondrial protein translocase assembly. Sci. Rep. *6*, 27484.

Yamamoto, H., Esaki, M., Kanamori, T., Tamura, Y., Nishikawa, Si., and Endo, T. (2002). Tim50 is a subunit of the TIM23 complex that links protein translocation across the outer and inner mitochondrial membranes. Cell *111*, 519–528.

STAR★METHODS

KEY RESOURCES TABLE

REAGENT or RESOURCE	SOURCE	IDENTIFIER
Antibodies		
Rabbit Polyclonal anti-Tim23	Chacinska et al., 2005	236-6
Rabbit Polyclonal anti-Tim50	Geissler et al., 2002	257-7
Rabbit Polyclonal anti-Pam17	van der Laan et al., 2005	3886-2
Rabbit Polyclonal anti-Tim44	Ieva et al., 2014	1835-4
Rabbit Polyclonal anti-mtHsp70	Ieva et al., 2014	1830-4
Rabbit Polyclonal anti-Pam18	Chacinska et al., 2005	751-4
Rabbit Polyclonal anti-Tim17	Chacinska et al., 2005	1845-3
Rabbit Polyclonal anti-Atp19	Gebert et al., 2012	1960-1
Rabbit Polyclonal anti-Rip1	Ieva et al., 2014	543-5
Rabbit Polyclonal anti-Tim21	Ieva et al., 2014	258-7
Rabbit Polyclonal anti-Tom70	Gebert et al., 2012	657-7
Rabbit Polyclonal anti-Mgr2	Gebert et al., 2012	3121-5
Rabbit Polyclonal anti-Tom40	Ieva et al., 2014	168-7
Rabbit Polyclonal anti-Tim22	Gebert et al., 2012	164-8
Rabbit Polyclonal anti-Cox4	Gebert et al., 2012	578-5
Rabbit Polyclonal anti-Mgm1	Ieva et al., 2014	796-4
Anti-Rabbit IgG-Peroxidase Antibody Produced in Goat	Sigma	Cat#A6154
Peroxidase Anti-Peroxidase Soluble Complex Antibody Produced in Rabbit	Sigma	Cat#P1291
IgGs from Human Serum	Sigma	Cat#I4506
Chemicals, Peptides, and Recombinant Proteins		
3,3′-Dipropylthiadicarbocyanine iodide $DiSC_3(5)$	Sigma	Cat#43608
Antimycin A	Sigma	Cat#A8674
Valinomycin	Sigma	Cat#V0627
Oligomycin	Sigma	Cat#O4876
Methotrexate	Sigma	Cat#A6770
Apyrase	Sigma	Cat#A7646
AcTEV™ Protease	Fisher Scientific	Cat#10443432
Protino® Ni-NTA Agarose	Macherey-Nagel	Cat#745400
CNBr-Activated Sepharose 4B	GE Healthcare	Cat#17043001
L-[^{35}S-Methionine	Hartmann Analytic	Cat#SCM-01
Critical Commercial Assays		
TNT® SP6 Quick Coupled Transcription/Translation System	Promega	Cat#L2080
In-Fusion® HD Cloning Kit	Takara	Cat#639649
PrimeSTAR® Max DNA Polymerase	Takara	Cat#R045A
Experimental Models: Organisms/Strains		
YPH499 (wild-type) *MATa ura3-52 lys2-801_amber ade2-101_ochre trp1-Δ63 his3-Δ200 leu2-Δ1*	Sikorski and Hieter, 1989	R20(1501)
YPH499 *tim50::ADE2* p*TIM50*	Wenz et al., 2014	R1(2993)
YPH499 *tim50::ADE2* p*tim50*$^{TM/IMS}$	This paper	R175
YPH499 *tim50::ADE2* p*tim50*^{IMS}	This paper	R176
YPH499 *tim50::ADE2* p*tim50-7*	Wenz et al., 2014	R2(2994)
YPH499 *tim23::HIS3-PNOP1-PA-TIM23*	Geissler et al., 2002	R76(2802)

(*Continued on next page*)

Continued

REAGENT or RESOURCE	SOURCE	IDENTIFIER
YPH499 *tim23::HIS3-PNOP1-PA-TIM23 tim50::ADE2* p*TIM50*	This paper	R177
YPH499 *tim23::HIS3-PNOP1-PA-TIM23 tim50::ADE2* p*tim50*$^{TM/IMS}$	This paper	R178
YPH499 *tim23::HIS3-PNOP1-PA-TIM23 tim50::ADE2* p*tim50*^{IMS}	This paper	R179
YPH499 *tim23::HIS3-PNOP1-PA-TIM23 tim50::ADE2* p*tim50-7*	This paper	R180
YPH499 *pam17::HIS5*	van der Laan et al., 2005	R122(1620)
YPH499 pRS426	This paper	R181
YPH499 pACS1	This paper	R182
PK82 (wild-type) *MATα his4-713 lys2 ura3-52 Δtrp1 leu2-3,112*	Gambill et al., 1993	R36(2501)
PK83 *MATα ade2-101 lys2 ura3-52 leu2-3,112 Δtrp1 ssc1-3 (LEU2)*	Gambill et al., 1993	R38(2503)
Oligonucleotides		
pACS2-fw	AGAGAAAAGTATGCTAACTGG	Tim50-fw2
pACS2-rev	TGTAAGAATGGATTTAGGCTTGTC	Tim50-rev2
pACS3-tim50-fw	GCAAGGGATTGGGAGCCT	Tim50-fw1
pACS3-tim50-rev	TAAAATGGACAGCAT	Tim50-rev1
pACS3-b2-fw	ATGCTGTCCATTTTACTAAAATACA AACCTTTACTAAAAATC	cyb2fus1
pACS3-b2-rev	AGGCTCCCAATCCCTTGCGGATCC TTGAAGGGGACCCA	cyb2fus2
pACS1-Tim50-fw	GAATTCGCGGGGGATCTCCCATG	pPGK-fw1
pACS1-Tim50-rev	TTCTTCAGACTCTTGAGGCTC	IMS-rev1
pACS1-PA-fw	TCAAGAGTCTGAAGAAGGATCCG AGAATCTTTATTTTCAG	Tevfw1
pACS1-PA-rev	GATCCCCCGCGAATTCTCAGGAA TTCGCGTCTACTTTC	protArev1
Recombinant DNA		
pGEM4Z-Cyt1 (*S. cerevisiae*)	Geissler et al., 2002	C06
pGEM4Z-Tim44 (*S. cerevisiae*)	This paper	T44
pGEM4Z-Atp2 (*S. cerevisiae*)	Geissler et al., 2002	F01
pGEM4Z-Pam18 (*S. cerevisiae*)	This paper	P18
pGEM4Z-AAC (*S. cerevisiae*)	Ryan et al., 1999	A01
pGEM4Z-b_2(167)-DHFR (Cyb2 (*S. cerevisiae*)-DHFR (mouse))	Geissler et al., 2002	BO3
pGEM4Z-$b_2(167)_\Delta$-DHFR (Cyb2 (*S. cerevisiae*)-DHFR (mouse))	Geissler et al., 2002	BO4
pGEM4Z-b_2(220)-DHFR (Cyb2 (*S. cerevisiae*)-DHFR (mouse))	Geissler et al., 2002	B18
pRS426	Christianson et al., 1992	N/A
p*TIM50* (*S. cerevisiae*)	Wenz et al., 2014	N/A
p*tim50*$^{TM/IMS}$ (*S. cerevisiae*)	This paper	pACS2
p*tim50*^{IMS} (*S. cerevisiae*)	This paper	pACS3
p*tim50-7* (*S. cerevisiae*)	Wenz et al., 2014	N/A
p*tim50*$^{MX/TM-PA}$ (Tim50 (*S. cerevisiae*)-Protein A (*S. aureus*))	This paper	pACS1
Software and Algorithms		
Multi Gauge v.3.0	FujiFilm	N/A

LEAD CONTACT AND MATERIALS AVAILABILITY

Information and requests for reagents and resources unique to this study should be directed to and will be fulfilled by the Lead Contact, Raffaele Ieva (raffaele.ieva@ibcg.biotoul.fr). Reagents generated in this study will be made available on request but we may require a completed Material Transfer Agreement if there is potential for commercial application.

EXPERIMENTAL MODEL AND SUBJECT DETAILS

Yeast (*S. cerevisiae*) strains used in this study and their genotypes are described in the KEY RESOURCES TABLE. *S. cerevisiae* strains were cultured in yeast peptone media (1% [w/v] yeast extract, 2% [w/v] Bacto peptone) supplemented with either 3% [w/v] glycerol (YPG) or 2% [w/v] dextrose (YPD), or in synthetic defined medium containing 0.67% (w/v) Difco-yeast nitrogen base, a dropout amino acid mix and 3% (w/v) glycerol, or 2% (w/v) dextrose, or 2% lactate and 0.1% dextrose. Yeast cultures were conducted at temperatures ranging between 17°C and 37°C as described in the Method Details and in Figure Legends.

METHOD DETAILS

Yeast Strains, Plasmids and Growth Conditions

Mutant strains were generated from *S. cerevisiae* YPH499 (*MAT*a, *ade2-101, his3-Δ200, leu2-Δ1, ura3-52, trp1-Δ63, lys2-801*) (Sikorski and Hieter, 1989). To generate temperature-sensitive *tim50* mutant strains, *tim50* alleles obtained by error-prone PCR or the wild-type *TIM50* gene were cloned into the centromeric plasmid pFL39. The obtained pFL39-derivative plasmids were transformed by plasmid shuffling into a *tim50* deletion strain, where the open reading frame of *TIM50* had been previously replaced with the *ADE2* cassette using homologous recombination. Transformants were tested for growth at 24°C, 30°C and 37°C both on fermentative and respiratory media. The sequence of the *tim50-7* allele (Wenz et al., 2014), amplified from the corresponding mutant strain, encodes the amino acid substitutions V289A, K363E, E400G, K435N, I451V. The pFL39 derivative plasmid containing the wild-type *TIM50* gene was also used as a template to generate *tim50* truncation alleles. The plasmid harboring the *tim50*$^{TM/IMS}$ allele was obtained by inverse PCR. The plasmid harboring *tim50*^{IMS} was obtained by In-Fusion Cloning (Takara) using a construct encoding the *S. cerevisiae* Cyb2 amino acid sequence 2-167 (amplified from plasmid B18, see below) which was fused in between codons 5 and 132 of the Tim50 encoding sequence. Both alleles were transformed by plasmid shuffling into a *tim50* deletion strain as described above. To generate *tim50* mutant strains that express a N-terminally protein A-tagged form of Tim23, a construct encoding a *HIS3* selection cassette, the *NOP1* promoter, and a tandem protein A sequence followed by the cleavage site for the tobacco etch virus (TEV) protease was fused to the second codon of chromosomal *TIM23* using homologous recombination (Geissler et al., 2002). A strain expressing both wild-type Tim50 and the protein A-tagged Tim50$^{Mx/TM}$ was obtained by transforming YPH499 with pACS1. This multicopy plasmid harbors the *PGK1* promoter and terminator regions flanking an open reading frame that encodes the first 142 residues of Tim50 fused via the TEV protease cleavage site to a tandem protein A sequence. YPH499 transformed with the multicopy empty vector pRS426 was used as a control reference strain expressing only the wild-type copy of *TIM50*. The *pam17*Δ and *ssc1-3* strains were previously described (Gambill et al., 1993; van der Laan et al., 2005).

Mitochondria Isolation, Analysis of Protein Content and Mitochondrial Δψ Measurement

To isolate mitochondria, all strains were cultured in glycerol-containing media at 24°C, except the strain *ssc1-3,* which was grown at 17°C. Collected cells were subjected to enzymatic digestion of the cell wall and mechanical disruption of the plasma membrane. Mitochondria were subsequently isolated using differential centrifugation (Meisinger et al., 2006). The mitochondrial protein content was solubilized in Laemmli buffer (2% [w/v] SDS, 10% [w/v] glycerol, 60 mM Tris-HCl, pH 6.8, 0.01% [w/v] bromophenol blue, 2 mM phenylmethylsulfonyl fluoride [PMSF], 1% [v/v] 2-mercaptoethanol) and denatured at 95°C for 5 min. Proteins were separated by NuPAGE (Thermo Fisher Scientific) polyacrylamide gel electrophoresis, transferred onto a PVDF membrane and decorated with specific antisera. The mitochondrial Δψ was measured by monitoring the fluorescence of the potential sensitive dye 3,3′-dipropylthiadicarbocyanine iodide ($DISC_3(5)$) using a fluorometer with excitation and emission wavelengths set to 622 nm and 670 nm, respectively. The response time was set to 1 s, the slit width was 5 nm. Mitochondria were diluted to a concentration of 20 μg/ml into a cuvette containing 3 mL of Δψ-measurement buffer (0.6 M sorbitol, 10 mM $MgCl_2$, 0.5 mM EDTA, 20 mM KPi, pH 7.2, 0.1% [w/v] bovine serum albumin [BSA], 5 mM malate, 5 mM succinate) with the addition of 2 μM $DISC_3(5)$. Upon uptake and quenching of the $DISC_3(5)$ fluorescence, samples were supplemented with 1 μM valinomycin to uncouple the membrane potential. The gain of fluorescence measured upon uncoupling was used to estimate the degree of mitochondrial Δψ accumulation in different mitochondrial samples. Where indicated, *in vitro* heat shock of isolated mitochondria was conducted prior to measurements, by incubating 200 μL of Δψ-measurement buffer containing 60 μg of mitochondria at 37°C for 15 min. This reaction was added to a cuvette containing 2.8 mL of Δψ-measurement buffer and 2 μM $DISC_3(5)$ at room temperature. In all cases, fluorescence measurements were conducted at 25°C.

In Vitro Preprotein Synthesis and Import into Isolated Mitochondria

A series of pGEM4Z-derivative plasmids, containing genes under the transcriptional control of the SP6 promoter, that encode respectively b_2(167)-DHFR (B03), $b_2(167)_\Delta$-DHFR (B04), b_2(220)-DHFR (B18), Atp2 (F01), Cyt1 (C06), AAC (A01), Tim44 (T44), and Pam18 (P18), were used. For *in vitro* synthesis and radiolabeling of precursor proteins, the pGEM4Z-derived plasmids were added to the SP6 TNT Quick Coupled transcription/translation rabbit reticulocyte lysate system (Promega) in the presence of [^{35}S]methionine. Isolated mitochondria were diluted in import buffer (3% [w/v] BSA, 250 mM sucrose, 80 mM KCl, 5 mM $MgCl_2$, 2 mM KH_2PO_4, 5 mM methionine, 10 mM, MOPS-KOH, pH 7.2), and supplemented with 2 mM ATP, 2 mM NADH as well as an ATP regenerating system (5 mM creatine phosphate, 0.1 mg/ml creatine kinase). Mitochondria were supplemented with an AVO mix (8 μM antimycin

A, 1 μM valinomycin, 20 μM oligomycin) (−Δψ reactions) or an identical volume of ethanol (+Δψ reactions). Import reactions were started by the addition of lysate containing radiolabeled proteins to mitochondria and stopped by adding the AVO mix (+Δψ reactions) or an identical volume of ethanol (−Δψ reactions). All reaction mixtures were then cooled on ice. Samples were split into two equal aliquots, one of which was supplemented with 50 μg/ml Proteinase K for 15 min on ice. The protease was then inactivated using 2 mM PMSF. Where indicated, heat shock was conducted prior to import by incubating mitochondria in import buffer at 37°C for 5 min (*ssc1-3*) or 15 min (*tim50-7*). To assess the import-driving activity exerted by the PAM machinery, radiolabeled $b_2(167)_\Delta$-DHFR was first supplemented with 5 μM methotrexate (MTX) for 5 min at 25°C to stabilize the folding of the DHFR moiety. This preparation of $b_2(167)_\Delta$-DHFR was added to mitochondria diluted in import buffer containing 5 μM MTX, 2 mM ATP, 2 mM NADH, 5 mM creatine phosphate and 0.1 mg/ml creatine kinase. After a first incubation time of 15 min, an aliquot corresponding to a third of each reaction was withdrawn and cooled on ice (Δt = 0 min, +Δψ, − Proteinase K). The remaining two thirds of the reactions were supplemented with 1 μM valinomycin and incubated at 25°C for the indicated chase time, prior to digestion with 50 μg/ml Proteinase K for 15 min on ice (Δt = 3 min and Δt = 15 min, −Δψ, + Proteinase K). After protease inactivation with 2mM PMSF, mitochondria were re-isolated. The protein content of mitochondria subjected to import reactions was solubilized using a denaturing protocol as described above, except in the case of ADP/ATP carrier (AAC) import. AAC import reactions were subjected to Proteinase K digestion, prior to re-isolation of mitochondria and analysis by blue native gel electrophoresis to resolve radiolabeled AAC (Palmisano et al., 1998; Ryan et al., 1999). To this end, mitochondria were gently resuspended in ice-cold digitonin buffer (20 mM Tris-HCl, pH 7.4, 10% [w/v] glycerol, 50 mM NaCl, 0.1 mM EDTA, 1 mM PMSF), containing 1% (w/v) digitonin, and incubated on ice for 15 min. After a clarifying centrifugation step, solubilized proteins were separated on a 6%–16.5% acrylamide blue native gel. All radiolabeled proteins were detected by autoradiography using a Storm phosphorimager (GE Healthcare) and processed using the MultiGauge software (FujiFilm). Removal of non-relevant gel lanes is indicated by white spaces separating the adjacent parts of the gels shown in the figures.

Native Isolation of Protein Complexes by IgG Affinity Purification

IgG affinity chromatography was conducted adapting previously established protocols (Geissler et al., 2002; Truscott et al., 2003; Chacinska et al., 2005; van der Laan et al., 2005; van der Laan et al., 2007). Isolated mitochondria were solubilized in buffer containing 1% (w/v) digitonin, for 30 min at 4°C. After removing the insoluble material by centrifugation, the supernatant was incubated with IgG-Sepharose beads. Samples were mixed by agitation for 1.5 h at 4°C to allow binding of the protein A tag to immobilized IgGs. After extensive washes of the resin with buffer containing 0.3% (w/v) digitonin, bound proteins were eluted using either ammonium acetate or TEV protease (Thermo Fisher). Where indicated, mitochondria were subjected to ATP depletion or supplemented with ATP prior to solubilization. To this end, mitochondria were diluted in import buffer to 1 mg/ml and supplemented with 20 μM oligomycin, 0.2 Units/ml apyrase and incubated at 25°C for 15 min. After re-isolation, mitochondria were resuspended in import buffer, supplemented with 20 μM oligomycin, 2 mM NADH and divided in two aliquots. One aliquot (−ATP) was directly incubated at 25°C for 10 min. The other aliquot (+ATP) was supplemented with 2 mM ATP, 5 mM creatine phosphate and 0.1 mg/ml creatine kinase and incubated at 25°C for 10 min. This incubation was followed by solubilization of protein contents with digitonin as described above.

QUANTIFICATION AND STATISTICAL ANALYSIS

To quantify signal intensities, the MultiGauge (Fujifilm) analysis software was used. For import experiments, signals were normalized to those obtained for the reference wild-type sample at the longest time point. The import-driving force generated by the import motor on $b_2(167)_\Delta$-DHFR was estimated by quantifying the fraction of Proteinase K-resistant intermediate form of the accumulated preprotein, i-$b_2(167)_\Delta$-DHFR, obtained after the indicated chase time (Δt). Values were normalized to the amount of i-$b_2(167)_\Delta$-DHFR generated during the first incubation (Δt = 0 min, + Δψ, − Proteinase K). The intensities of bands corresponding to proteins co-eluted with IgG affinity purified Tim23 were normalized to the relative amount of yielded bait protein. In all graphs, the error bars represent the standard error of the mean (SEM) obtained from a number (n) of independent experiments as indicated in the Figure Legends.

DATA AND CODE AVAILABILITY

This study did not generate any unique datasets or code.